REPUBLIC OF TURKEY
ADANA ALPARSLAN TÜRKEŞ SCIENCE AND TECHNOLOGY UNIVERSITY

GRADUATE SCHOOL OF NATURAL AND APPLIED SCIENCES
DEPARTMENT OF ELECTRICAL AND ELECTRONIC ENGINEERING

MODELING and REALIZATION of DRY TYPE TRANSFORMER with OPTIMUM WEIGHT and EFFICIENCY CHARACTERISTICS

BURAK ESENBOĞA
MASTER OF SCIENCE

ADANA 2019

REPUBLIC OF TURKEY

ADANA ALPARSLAN TÜRKEŞ SCIENCE AND TECHNOLOGY UNIVERSITY

GRADUATE SCHOOL OF NATURAL AND APPLIED SCIENCES

DEPARTMENT OF ELECTRICAL AND ELECTRONIC ENGINEERING

MODELING and REALIZATION of DRY TYPE TRANSFORMER with OPTIMUM WEIGHT and EFFICIENCY CHARACTERISTICS

BURAK ESENBOĞA

MASTER OF SCIENCE

SUPERVISOR

ASST. PROF. DR. TUĞÇE DEMİRDELEN

ADANA 2019

MODELING and REALIZATION of DRY TYPE TRANSFORMER with OPTIMUM WEIGHT and EFFICIENCY CHARACTERISTICS

submitted by **Burak ESENBOĞA** in partial fulfillment of the requirements for the degree of **Master of Science in Department of Electrical and Electronic Engineering, Adana Alparslan Türkeş Science and Technology University** by,

Assoc. Prof. Dr. Gözde Baydemir PEŞİNT
Graduate School Director

Asst. Prof. Dr. Tuğçe DEMİRDELEN
Deputy Department Chair

Asst. Prof. Dr. Tuğçe DEMİRDELEN
Supervisor

Thesis Committee

Asst. Prof. Dr. Tuğçe DEMİRDELEN
Adana Alparslan Türkeş Science and Technology University

Asst. Prof. Dr. Murat Mustafa SAVRUN
Adana Alparslan Türkeş Science and Technology University

Asst. Prof. Dr. Ercan AVŞAR
Çukurova University

Thesis Defense Date

01/08/2019

I hereby declare that all information in this thesis has been obtained and presented in accordance with academic rules and ethical conduct. I also declare that, as required by these rules and conduct, I have fully cited and referenced all information that is not original to this work.

[Signature]

Burak ESENBOĞA

ABSTRACT

MODELING and REALIZATION of DRY TYPE TRANSFORMER with OPTIMUM WEIGHT and EFFICIENCY CHARACTERISTICS

Burak ESENBOĞA

Department of Electrical and Electronic Engineering

Supervisor: Asst. Prof. Dr. Tuğçe DEMİRDELEN

August 2019, 91 pages

When compared to the oil-filled transformers, dry type transformers are widely used in power distribution systems due to their non-flammable characteristic, high electrical strength against short circuits, easy maintenance and superior environmental performance. However, the thermal behavior of these transformers is undesirable since they have the natural cooling mechanism and operate at high temperatures in the distributed power systems. Moreover, the dry type transformers need the larger coils compared to oil-filled transformers with the same capacity ratings due to requiring a better insulating system. This case results in higher costs. Therefore, the main aim of this thesis is to design and produce a 3-phase dry-type transformer based on optimum weight and efficiency.

Firstly, a mathematical model of a 3-phase dry-type transformer is obtained taken in the account of the transformer's design parameters and losses in the core and windings. Secondly, this transformer is optimized by using Particle Swarm Optimization (PSO) method, one of the most preferred optimization methods in the literature. Thirdly, the transformer is designed by using it's the optimization parameters in ANSYS/Maxwell program so electromagnetic and thermal analysis of the transformer is performed. Finally, the transformer which is optimized, designed and analyzed efficiently is manufactured in the lower weight and higher efficiency. The manufactured transformer is also tested in the laboratory. Thus, the designed transformer is also verified experimentally. It is hoped that this thesis will contribute to the researchers and transformer manufacturing industries dealing with the optimum design, electromagnetic and thermal analysis of the 3-phase dry type transformers.

Keywords: ANSYS/Maxwell, dry type transformer, electromagnetic, thermal, optimization, modeling.

ÖZET

OPTİMUM AĞIRLIK VE VERİMLİLİK ÖZELLİKLERİNE SAHİP KURU TİP TRANSFORMATÖRÜN MODELLENMESİ VE GERÇEKLEŞTİRİLMESİ

Burak ESENBOĞA
Elektrik Elektronik Mühendisliği Anabilim Dalı
Danışman: Dr. Öğr. Üyesi Tuğçe DEMİRDELEN
Ağustos 2019, 91 sayfa

Yağ ile doldurulmuş transformatörlere kıyasla kuru tip transformatörler yanmaz özelliği, kısa devrelere karşı yüksek elektrik dayanımı, kolay bakımı ve üstün çevre performansı nedenleriyle güç dağıtım sistemlerinde yaygın olarak kullanılmaktadır. Ancak, bu transformatörlerin ısıl davranışları, doğal soğutma mekanizmasına sahip olduklarından ve dağıtık güç sistemlerinde yüksek sıcaklıklarda çalıştıklarından istenmeyen bir durumdadır. Ayrıca, kuru tip transformatörler, daha iyi yalıtım sistemi gerektirdiğinden, aynı kapasitede yağ dolu transformatörlere kıyasla daha büyük bobinlere ihtiyaç duyar. Bu durum daha yüksek maliyetlerle sonuçlanmaktadır. Bu nedenle, bu tezin asıl amacı, optimum ağırlık ve verime dayalı 3 fazlı kuru tip transformatör tasarlamak ve üretmektir. İlk olarak, transformatörün tasarım parametreleri, çekirdek ve sargılardaki kayıplar hesaba katılarak 3 faz kuru tip bir transformatörün matematiksel bir modeli elde edilmiştir. İkinci olarak, literatürde en çok tercih edilen optimizasyon yöntemlerinden biri olan Parçacık Sürü Optimizaston (PSO) yöntemi kullanılarak optimize edilmiştir. Üçüncüsü, transformatörün optimizasyon parametreleri kullanılarak transformatör ANSYS/Maxwell programında tasarlanmıştır, böylece transformatörün hem elektromanyetik hem de termal analizi yapılmıştır. Son olarak, verimli bir şekilde optimize edilen, tasarlanan ve analiz edilen transformatör, daha düşük ağırlık ve daha yüksek verimlilikte üretilmiştir. Üretilen transformatör labaratuvarda test edilmiştir. Böylece, tasarlanan transformatör deneysel olarak da doğrulanmıştır. Bu tezin, 3 faz kuru tip transformatörlerin optimum tasarımı, elektromanyetik ve termal analizi ile ilgilenen araştırmacılara ve transformatör üretim endüstrilerine katkıda bulunacağı ümit edilmektedir.

Anahtar Kelimeler: ANSYS/Maxwell, kuru tip transformatör, elektromanyetik, termal, optimizasyon, modelleme.

Dedication

I would like to dedicate my thesis to my beloved father.

ACKNOWLEDGEMENTS

In the preparation of this thesis, I would like to thank my esteemed adviser Asst. Prof. Dr. Tuğçe DEMİRDELEN who has always been exemplary of her knowledge, business approach, skills and a broad perspective.

I would also like to thank my committee members, Asst. Prof. Dr. Murat Mustafa SAVRUN, Asst. Prof. Dr. Ercan AVŞAR for letting my defense be an enjoyable moment, and for their brilliant comments and suggestions.

I would like to thank Asst. Prof. Dr. Fırat EKİNCİ, Res. Asst. Kemal AYGÜL, Res. Asst. Abdurrahman YAVUZDEĞER, Res. Asst. İnayet Özge AKSU and Res. Asst. Murat ÇIKAN for their valuable discussion and technical help.

Finally, I must express my very profound gratitude to my parents and to my brothers for providing me with unfailing support and continuous encouragement throughout my years of study and through the process of researching and writing this thesis. I would also like to thank my dear wife Mrs. Tuba ESENBOĞA who has motivated to me with patience, understanding and support.

This thesis was financially supported by the Scientific and Technological Research Council of Turkey (TÜBİTAK) with project number of 118E697 and the Scientific Project Unit of Adana Science and Technology University with project number 18332006.

TABLE OF CONTENTS

LIST OF FIGURES

LIST OF TABLES

NOMENCLATURE

AC	: Alternating Current
DC	: Direct Current
NARX	: Nonlinear Autoregressive (NARX)
ELRN	: Elman Recurrent Networks
FEM	: Finite Element Method
IWO	: Invasive Weed Optimization
FA	: Firefly Algorithm
PSO	: Particle Swarm Optimization
ABC	: Artificial Bee Colony
CFD	: Computational Fluid Dynamics
LV	: Low Voltage
HV	: High Voltage
GSA	: Gravitational Search Algorithm
VPI	: Vacuum Pressure Impregnated
VPE	: Vacuum Pressure Encapsulated
Pbest	: Personal Best
Gbest	: Global Best
FEA	: Finite Element Analysis
Rmxprt	: Rotation Machinery Expert
PLC	: Programmable Logic Controller
CPU	: Central Processing Unit
RAM	: Random Access Memory
ROM	: Read only Memory
EPROM	: Erasable Programmable Read Only Mem
HMI	: Human Machine Interface
A/D	: Analog/Digital
I/O	: Input / Output
V/I	: Voltage / Current
MgO	: Magnesium Oxide
IEEE	: Institute of Engineers and Everyone Else

e_1	: Induced Voltage
U_1	: Primary Winding Instantaneous Voltage Value
ϕ_m	: Magnetic Flux
$\phi_{\max}$	: Peak of The Total Magnetic Flux
f	: Frequency
w	: Angular Velocity
N	: Number of Turn
n	: Turn Ratio
I	: Current
R_1	: Primary Winding Resistance
X_1	: Primary Winding Reactance
R_2	: Secondary Winding Resistance
X_2	: Secondary Winding Reactance
I_c	: Core Loss Current
I_m	: Magnetization Loss Current
B	: Flux Density
H	: Magnetizing Force
∇	: Gradient Operator
K	: Thermal Conductivities of the Transformer
Q	: Internal Heat Generation Per Unit Area in Transformer
e	: Unit Vectors
E	: Electric Field Intensity
H	: Magnetic Field Intensity
D_a	: Electric Flux (Displacement) Density
J	: Conduction Current Density
ρ	: Source Charge Density
S	: Apparent Power
C	: Transformer Core Section Acceptability
D	: Diameter of a Leg of the Transformer Core
q_{fej}	: Yoke cross-section of the core leg

q_{fe}	: Cross-Section of the Core Leg
B_j	: Yoke Induction of the Core Leg
q_1	: HV Windings Cross-Section of the Transformer
q_2	: LV Windings Cross-Section of the Transformer
s	: Current Density of the Windings
L_s	: Window Height of the Core
A_s	: Specific Ampere Winding
w_1	: Primary Windings Number of Turn of the Transformer
w_2	: Secondary Windings Number of Turn of the Transformer
k_{cu}	: Window Copper Filling Factor
l_{m1}	: Average lengths of HV windings
l_{m2}	: Average lengths of LV windings
G_{cu1}	: Weight of The HV Windings
G_{cu2}	: Weight of The LV Windings
γ_{cu}	: Copper-Specific Weights
r	: winding resistance
P_{cu}	: Copper Losses
k	: Resistance Increase Factor
P_{feb}	: Iron Loss for Each of the Three Legs
P_{fej}	: Iron Loss for The Yoke
G_{feb}	: Weight of 3 Legs of the Transformer Core
γ_{fe}	: Iron Specific Weight Constant
G_{fej}	: Weight of the Transformer Yoke
p_{fej}	: Specific yoke iron loss in the transformer core

p_{fe}	: Leg Iron Loss in the Transformer Core
ξ_2	: Loss Factor
p_{10}	: Additional Loss Factor of the Core
G_{total}	: Total Weight of the Transformer
η	: Efficiency
x	: Particle Value
v_i^n	: Velocity of the ith Particle in the nth Iteration
c_1	: Social Parameter
c_2	: Cognitive Parameter
y	: Restriction Factor

1. INTRODUCTION

Transmission and distribution of electrical energy in an economical way is one of the most important issues in the energy field. Transformers are the main components of the electric transmission and distribution networks since alternating current (AC) electric power is transmitted over the long distances from power plants to consumption centers and rural areas. With the help of the transformers, the transmission and distribution of electrical energy are facilitated and this energy has become more useful. Because of this reason, transformers have gained market share in various application areas that require high quality of safety, stability and reliability such as rural areas, hospitals and residential.

In recent years, there has been a notable increase in the type of transformers used for small and medium power applications. The most important types are oil-filled transformers, gas-insulated transformers and dry-type transformers. In many critical applications such as hospitals, airports, schools, marine ships, military and residential areas, transformers must be protected against the risks of burning and explosion. Therefore, non-flammable, safer and more environmental friendly transformers have been offered for the critical applications. Among various transformer technologies, dry-type transformers are currently suitable installation in such places with a high standard of safety and reliability. Because, they do not contain flammable or contaminant materials, have high dielectric strength against the short circuit cases, not the use of pollutant materials such as oil and not requiring maintenance.

However, one of the most important issues of dry-type transformers is that they are costly and heavy when compared to oil-filled transformers with the same voltage and capacity rating. Because dry-type insulation systems lack the additional cooling and insulating properties. In order to have a better insulation system and cooling efficiency, these transformers are produced as larger dimensions and need more materials than oil-filled transformers. Another issue is that overloading of dry-type transformers significantly influence transformers insulation deterioration as well as thermal aging and their remaining life. Moreover, poor heat conduction performance of dry-type transformers results in rising winding temperature, acceleration of insulation aging and huge economic losses. Thus, the dry-type transformer analysis has been quite crucial considering these two important issues.

In Part 2, the literature review presents the studies on dry-transformers performed in recent years. The studies consist of thermal or electromagnetic or optimization based analysis on the dry-type transformer. None of the studies have focused on both thermal/electromagnetic performance and weight/efficiency based analysis of dry-type transformers. Due to the limitations of present studies in the literature, the aim of this thesis is:

- to obtain the mathematical model of a 3-phase dry type by using transformer design parameters and losses in the core and windings.

- to optimize the transformer design based on weight and efficiency by applying effective optimization methods and algorithms.

- to model and perform both electromagnetic and thermal analysis of the transformer thanks to ANSYS/Maxwell program.

- to test and verify the simulation results with experimental results.

- to manufacture the 3-phase dry-type transformer in the lower weight and higher efficiency.

The major ideas of this thesis focus on these five aspect of the proposed system.

2. LITERATURE REVIEW

Researchers have performed many theoretical and experimental studies about dry-type transformers in order to optimize the cost, weight, efficiency and increase the lifetime against the insulation and thermal aging. Table 2.1 summarize the literature review of the experimental and theoretical analysis of the dry type transformers.

Azizian and Bigdeli (2017) presented two new dynamic thermal models based on Elman Recurrent Networks (ELRN) and the Nonlinear Autoregressive (NARX) neural networks for dry-type transformers. A special type of dry-type transformer was selected to investigate the temperature distribution. The neural networks were trained by using the gathered experimental data. The windings and cooling air in the transformer were predicted by comparing experimental and neural network based thermal models results. Results showed that thermal models exhibited accurate results to present a dynamic thermal model of a dry-type transformer.

Soltanbayev et al. (2017) focused on an online monitoring intelligent system that provides to predict the dry-type transformer aging rate and life reduction. The transformer was designed by using the design parameters. Thermal and hot-spot temperature analysis of the transformer was performed for different load and environmental condition. An algorithm was developed to predict the temperature distribution of the transformer and thermal aging rate. Moreover, the transformer loading capability was evaluated under different ambient temperature and insulation classes.

Basak et al. (2015) presented a design procedure in order to obtain optimum cost based a dry-type transformer. A number of turns and window width are the most important key parameters to calculate the cost of the transformers. Authors used these parameters as cost functions. Manufacturer’s data compared with obtained optimal design data. Results showed that a more efficient and cost-effective transformer was designed by using an optimal cost design algorithm.

Wang S., Wang Y. and Zhao (2015) analyzed winding hot spot temperature rate and insulation life losses of a dry-type transformer under rated load conditions. They conducted a hot-spot temperature calculation model to predict the insulation life loss of the dry-type transformers. This model was created by analyzing the average temperature rising of inner and outer surfaces of the LV winding. The average temperature rising of the transformer windings was established by the hot-spot temperature calculation model. The thermal and life loss calculation model was used to analyze the transformer. As a result, the highest temperature was observed at the low voltage winding of the transformer and life loss of the transformer was 2107.5 hours at the rated load condition.

Tören and Çelebi (2016) investigated how the core material used in the core of a dry-type transformer impact on the total loss of the transformer and its efficiency. It was obtained that the non-crystalline amorphous material is lower core losses than the other crystalline materials in the distribution type transformers. In reducing losses and increasing efficiency, it is seen that the use of materials with the reduced crystal structure and low thickness will give better results.

Smajic et al. (2017) presented an electromagnetic model of a dry-type transformer and performed the transient behavior under the overvoltage condition. Authors analyzed the frequency-dependent core of the transformer by using 2D Finite Element Method (FEM). This analysis provided to the protection of the transformer against uncommon transients experienced in real circumstances.

Chitaliya and Joshi (2016) studied on the prediction of the transformers’ temperature rises under the full load condition. 3D FEM method was used to analyze the temperature distribution in the core and windings of a 160 kVA dry-type transformer. Results showed that duct size and the air flow in between the winding should be increased in order to have better heat transfer in the transformer.

Xiao and Du (2016) investigated the effect of epoxy resin insulation material on the dry-type transformers’ windings. Authors conducted that epoxy resin materials have lower thermal conductivity. The thermal conductivity factor and dielectric breakdown strength directly related to the effect on the temperature rises. Thermal conductivity of the epoxy resin material was improved by using micro and nano BN composites. It was seen that temperature rises on the transformer are reduced by the epoxy/BN composite.

Aksu and Demirdelen (2018) studied on the dry-type transformer design for industrial application. Authors proposed Invasive Weed Optimization (IWO) and the Firefly Algorithm (FA) method in order to optimize the weight and cost of the transformer. Mathematical model of the dry-type transformer was obtained to calculate its design parameters. Current density and core quality factor were determined as constraints. The optimal results were obtained by comparing the results with meta-heuristic algorithms.

Azizian et al. (2016) presented a cast resin transformer optimization design with a genetic algorithm, particle swarm optimization (PSO) and artificial bee colony (ABC) methods. The optimization results were compared with the available design proposed by the manufacturer. Results showed that PSO and ABC algorithms give a better performance than the GA algorithm.

Finocchio et al. (2015) mentioned that the most important design variable is to evaluate the winding temperature and thermal quality of the dry-type transformers. With the help of the neural network method, obtained thermal data of the 300 dry-type transformers from the same manufacturer were trained. Winding and total losses of the transformers were also predicted. It was seen that the neural network works with excellent accuracy to estimate the winding temperature and losses of the transformers.

Subramaniam et al. (2015) focused on online thermal prognosis intelligent system examining transformer aging rate and insulation deterioration. A thermal model was developed by using real-time information including transformer remained thermal life. The thermal model was applied on the different insulation materials.

Eslamian et al. (2011) studied the thermal behavior of the cast resin dry-type transformer. the heat transfer problem in The transformer was analyzed by FEM in order to investigate the heat transfer problem. a 3D finite volume based CFD model was formed to simulate heat flow intensity in the windings. Simulation results were compared with the experimental data measured from an 800 kVA cast resin dry-type transformer.

Comparison results were shown that CFD model gives accurate results but FEM-based model enables accuracy for real design application in short solution time.

Arjona et al. (2014) presented a model used by the dry-type transformer manufacturer industries to find a better temperature distribution of the transformer windings. The proposed model would contribute to extending the life of the transformer. Temperature distribution of the core, LV and HV windings for the no-load and load condition test were performed by FEM.

Alonso et al. (2017) determined the safe working limits of a dry-type transformer by investigation of the thermal response of the transformer in different temperature and load scenarios. The transformer has 10 kVA apparent power and H-class insulation. The hot spot temperature of the transformer was obtained and simulated by using the CFD model. 32 case studies examined the transformer remained life under stable conditions for 8 different load regimes and 4 ambient temperatures. 9 case studies used to examine the failure time of the transformer for 9 different overload conditions.

Smolka and Nowak (2018) presented the thermal, fluid flow and electromagnetic analysis of a medium power dry-type transformer in order to observe the power losses in the coils and windings. With the help of the CFD, a 3D dry-type transformer geometric model was created to analyze the heat flow and temperature distribution of the transformer coils and the core. The transformer mathematical model was obtained to determine the design process and transformer operation so the transformer was analyzed numerically. Also, experimental analysis of the transformer such as short circuit, open circuit, and temperature flow analysis was performed to validate with the numerical model of the transformer.

Wu and Kern (2016) conducted a thermal network model and a CFD simulation model to predict the winding temperature rises of the dry-type transformer. The thermal network model was based on Fourier’s law for heat transfer and Ohm’s law for electric circuits. Accuracy of the models was validated by comparing the compared with heat-run test results.

Glotic et al. (2016) presented a FEM-based transformer model to examine the thermal behavior of transformers. The model provided the identification of transformer thermal parameters thanks to the Differential Evolution Optimization algorithm. Thermal parameters were obtained as a result of experimental analysis and model-calculated values. Results validated the accuracy of numerical and analytical calculations.

Ghazizadeh, Faiz and Oraee (2016) proposed an analytical approach to predict the load losses, ohmic loss and winding eddy current loss in each winding under non-linear load current by FEM method. Magnetic flux density distribution in LV and HV windings of the transformer was analyzed in detail. Analysis results were validated by the proposed analytical approach.

Liu et al. (2016) introduced a quasi-3D coupled-field method which is the ability to calculate energy loss of core and velocity distribution in a plane above the lower yoke. The model was applied to a dry-type transformer to analyze the temperature rise of windings. The electromagnetic analysis of the transformer was performed to calculate power loss in the core and examine the magnetic flux density of the transformer.

Aghmasheh, Rashtchi and Rahimpour (2018) presented a new method to predict the geometry of windings instead of electrical parameters such as inductances, capacitances and loss parameters of the circuit. The method used to the gray box methodology based on design geometry prediction. In addition, the PSO algorithm was used to obtain an optimum winding size.

Nabhani, Hodgson and Warnakulasuriya (2015) tested and analyzed a 1.2MVA single phase dry-type transformer to predict the temperature rises under the loading condition. The temperature rises were calculated by creating a thermal evaluation model. The temperature rises in both the core and windings in the 1.2MVA transformer were validated by experimental results.

Alcan, Öztürk and Özmen (2014) presented a Gravitational Search Algorithm (GSA) to obtain the maximum efficiency of the oil-filled and dry-type transformers. There was an increase in efficiency as the loading rate increased but this increase did not change after a certain point. As a result; It is understood that GSA is a viable and alternative method for efficiency optimization with the parameters it has found.

Table 2.1. A review of experimental and theoretical analysis of dry-type transformers in literature.

Analysis Type of A Dry-Type Transformer	**Application**	**Optimization or Analysis (Thermal-Electromagnetic) Method**
Thermal	• Temperature distribution of windings and air cooling prediction • Thermal conductivity effect of epoxy resin insulation material • Insulation life loss calculation • Prediction of the temperature rise under full load condition • Heat dissipation in the transformer core and windings • Thermal response of the transformer in different temperature and load scenarios. • Calculation of the energy loss of core and velocity distribution in a plane above the lower yoke. • The temperature rises core and windings in a developed transformer	➢ Hotspot temperature calculating model (Wang et al., 2015) ➢ 3D Finite Element Method (FEM) (Chitaliya and Joshi, 2016) (Arjona et al., 2014) ➢ ANSYS- FEM analysis (Xiao and Du, 2016) ➢ Mathematical model based thermal analysis method (Subramaniam et al., 2015) ➢ 3D finite volume based CFD-FEM (Eslamian et al., 2011), (Alonso et al., 2017), (Smolka and Nowak, 2018) ➢ Thermal Network Model- CFD (Wu and Kern, 2016), ➢ A quasi-3D coupled-field method (Liu et al., 2016) ➢ Thermal Evaluation Model (Nabhani, Hodgson and Warnakulasuriya, 2015)

Optimization (cost, efficiency and temperature based)	• Prediction of the dry-type transformer thermal aging rate and life reduction • Number of turns and window width • Winding temperature distribution • Weight and cost optimization • Core, winding and insulation based design optimization • Identification of transformer thermal parameters • Transformer winding size design and optimization • Obtaining the maximum efficiency point of the transformer at different loading conditions	➢ Elman Recurrent Networks (ELRN) and Nonlinear Autoregressive (NARX) (Azizian and Bigdeli, 2017) ➢ Computational Algorithm (Soltanbayev et al., 2017) ➢ Exhaustive and Multivariable Search Method (Basak et al., 2015) ➢ Firefly Algorithm and Invasive Weed Optimization (Aksu and Demirdelen, 2018) ➢ Genetic Algorithm, Particle Swarm Optimization (PSO) and Artificial Bee Colony (Azizian et al., 2016) ➢ Differential Evolution Optimization (Glotic et al., 2016) ➢ Particle Swarm Optimization (PSO) (Aghmasheh, Rashtchi and Rahimpour, 2018) ➢ Gravitational Search Algorithm (Alcan, Öztürk and Özmen, 2014)
Electromagnetic	• Efficiency effect of different core materials • Investigation of electromagnetic behavior of dry-type transformers under transient over-voltages • Winding and core losses calculation • Examine the electrical properties of the coils and core	➢ ANSYS Maxwell (Tören and Çelebi, 2016) ➢ 2D-Finite Element Method (FEM) (Smajic et al., 2017), (Ghazizadeh, Faiz and Oraee, 2016) ➢ Artificial Neural Network (Finocchio et al., 2015)

	• Analysis of transformer windings load losses, ohmic losses and winding eddy current losses	➢ 3-D Numerical Model (Smolka and Nowak, 2018)

3. MATERIALS AND METHODS

3.1. Transformers

The power plants are often located far away from the consumption centers due to their energy sources needed. For this reason, it is necessary to transfer the electrical energy from the energy production area to the consumption areas. The transformers are the key components for this transfer process. They are electrical machines used in AC power systems to transfer the AC voltage from one level to another by magnetic induction without changing the frequency. They have great importance in changing the voltage values for the transmission and distribution of electrical energy. They are used for both increase and decrease the voltage. It is used as an amplifier in power plant output and as a lowering in consumption centers. There are several types of transformers used in electric transmission and distribution power systems, buildings, hospitals, marines, underground installations etc. for different purposes. Thus, they can be classified according to their power rating, voltage, current, weight, type of cooling etc.

3.1.1. Classification of the transformers

As mentioned above, there are a variety of transformers available in the market. One of the most important issues is to choose the most appropriate transformer based on where and how you would want to use it. Therefore, transformers are classified according to their various characteristics such as cooling systems, a number of phases, working principle, winding status, cooling types, core types and winding types. These classifications can be summarized as shown in Figure 3.1.

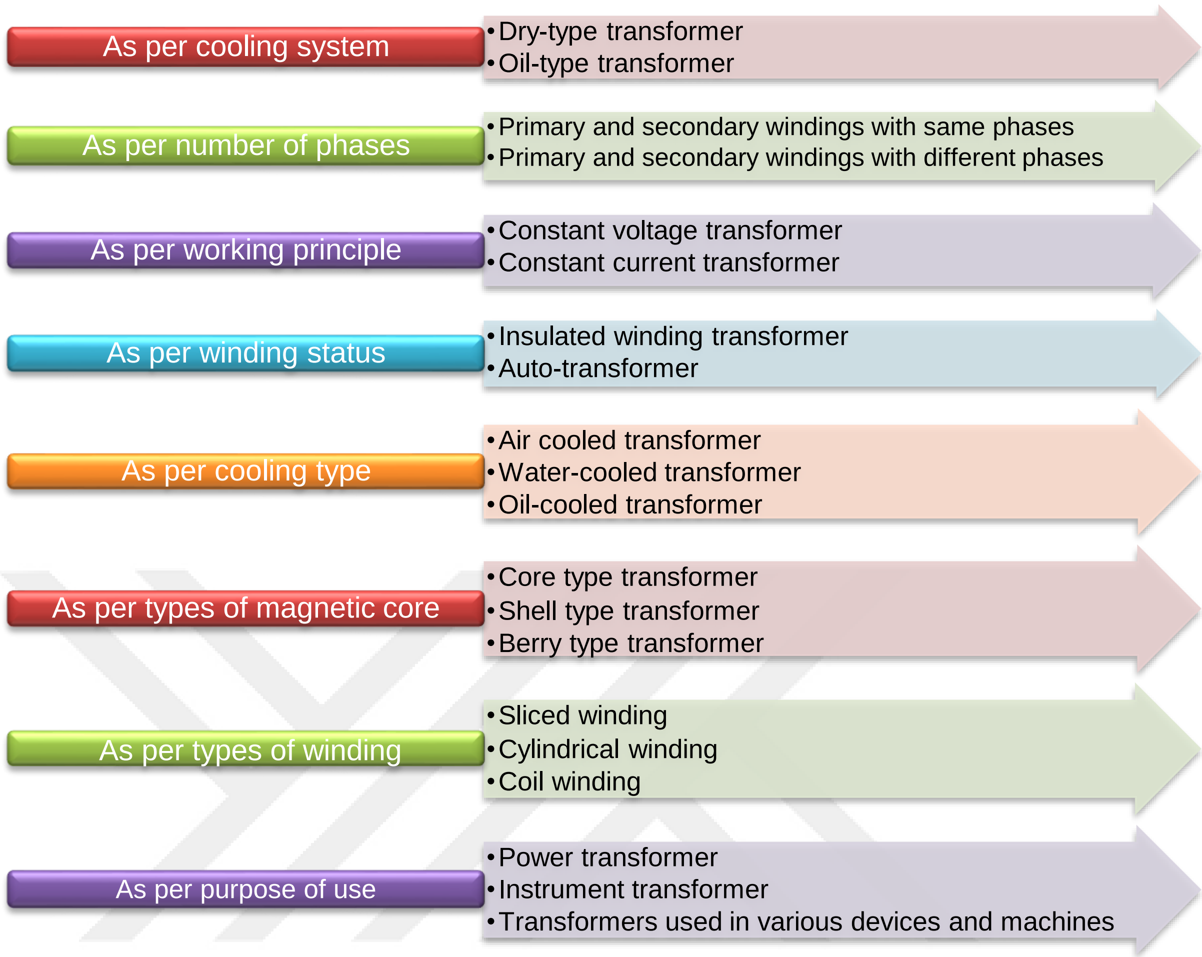

Figure 3.1. Classification of the transformers according to their various characteristics.

3.1.2. Working principle of the transformers

The transformers are basically electromagnetic devices that consist of a magnetic core and set of coils termed as primary and secondary windings. Primary and secondary windings have no electrical connection. The primary and secondary windings of the transformers are insulated from the magnetic core and also each other. Some materials such as press band, paper, mica, some plastics, various oils, cotton resins, tree wedges and stripboard are used as insulators. Figure 3.2 shows the working principle of a 1-phase transformer.

When the alternating voltage is applied to the transformers, an alternating current pass through the primary windings. This current creates a magnetic field that changes direction and intensity over the iron magnetic core according to time. This magnetic field completes the circuit by passing through the core and secondary winding and the electromagnetic motive force is induced in the secondary windings. Thus, the alternating voltage applied to the primary winding induces a voltage of the same frequency in the secondary winding by the electromagnetic induction principle.

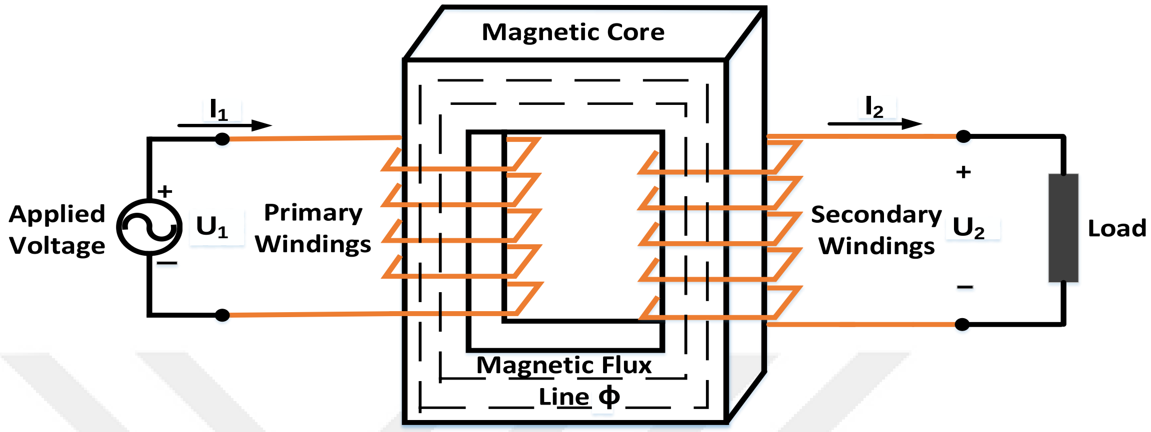

Figure 3.2. Working principle diagram of a 1-phase transformer.

When voltage is applied to the primary winding of the transformers, the magnetic field is formed, but since the magnetic field is not variable, the electromotive force is not induced in the secondary winding.

The induced voltage in the windings according to Faraday law;

$$e_1 = N_1 \frac{d\phi}{dt} \tag{1}$$

If the winding resistance value is accepted zero, then $U_1 = e_1$. In this case, since U_1 (primary winding instantaneous voltage value) changes in a sinusoidal, the value of ϕ_m is also variable according to the frequency of U_1.

$$\phi_m = \phi_{\max} \mathrm{sinwt} \tag{2}$$

Where $\phi_{\max}$ is the peak of the total magnetic flux and $w = 2\pi f$ (rad/sec.). If the value of ϕ_m is fulfilled in the Faraday Law;

$$e_1 = N_1 2\pi f \phi_{\max} \cos wt \tag{3}$$

Equation 2.4 shows that U_1, the effective (RMS) value of electromotive force induced in the primary winding, is obtained by dividing the peak value by two.

$$U_1 = \frac{1}{\sqrt{2}} N_1 2\pi f \phi_{\max} \cos wt = 4,44 N_1 f \phi_{\max} \cos wt \tag{4}$$

The induced voltage in the primary and secondary voltages of the transformer is expressed as shown in Equation 1 and 2.

$$U_1 = 4,44 N_1 f \phi_{\max} \cos wt \tag{5}$$

$$U_2 = 4,44 N_2 f \phi_{\max} \cos wt \tag{6}$$

There is a constant ratio between primary and secondary windings' numbers, voltages and currents of transformers. This ratio is called a turn ratio (n). Equation 3 shows the turn ratio formula related to the transformer's primary and secondary voltages, currents and number of turns.

$$n = \frac{U_1}{U_2} = \frac{N_1}{N_2} = \frac{I_2}{I_1} \tag{7}$$

N_1 and N_2 are the primary and secondary turn numbers, f is the system frequency, ϕ is the magnetic flux passing through the core and windings, I_1 and I_2 are the primary and secondary windings and K is the turn ratio of the transformer.

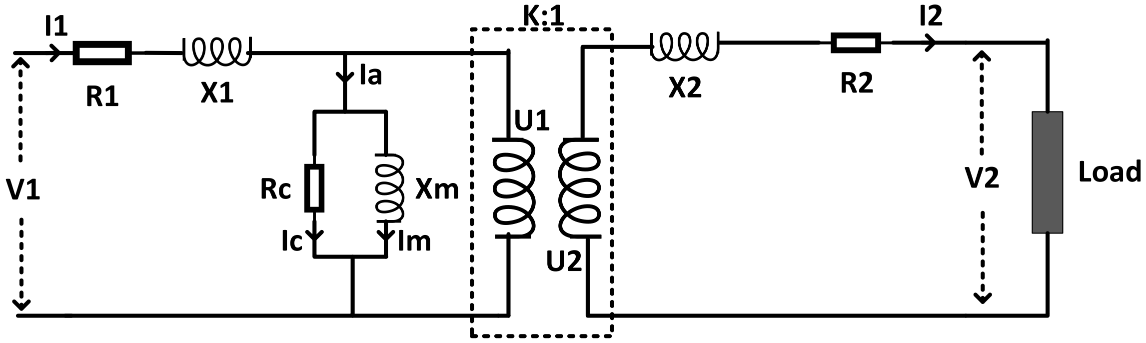

Figure 3.3. Equivalent circuit of the transformer.

Figure 3.3 presents the equivalent circuit of the transformer. Here, R_1 and X_1 are the primary winding resistance and reactance, respectively, and R_2 X_2 are secondary winding resistance and reactance. I_c and I_m are core loss current and magnetization loss current.

3.1.3. Transformer losses

Transformers are the static devices so there is no loss of friction and wind losses. However, there are various types of losses in the transformers. Figure 3.4 shows the transformer losses that are iron losses, copper losses, hysteresis losses, eddy current losses, stray loss and dielectric losses. These losses are originated from a variation of the magnetization in the windings and core of the transformer.

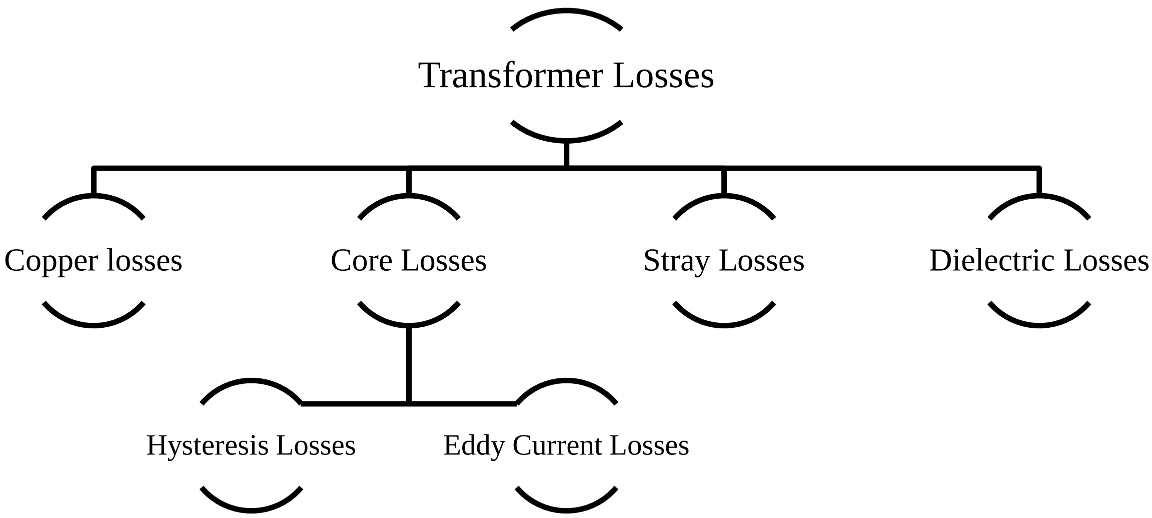

Figure 3.4. Types of losses in the transformer.

3.1.3.1. Copper losses

When a load is connected in the secondary side of the transformer, a current pass through both the primary and secondary windings. These currents create heat losses due to the resistance of the primary winding (R_1) and secondary winding (R_2). Therefore, copper losses in the transformers are caused by current passing through transformer windings. These losses are directly proportional to the resistance of the coils used in the winding and the square of the current passing through the coils. Total copper losses are expressed as Equation 8.

$$P_{total\_copper\_losses} = I_1^2 R_1 + I_2^2 R_2 \tag{8}$$

3.1.3.2. Core losses

When a voltage is applied to the transformer, un-loaded losses occur in the core of the transformer. The un-loaded losses are measured by open circuit operation of the transformer secondary side. These losses are also called as iron losses. These type of losses are divided into two groups: hysteresis and eddy current loss.

The electrons of the core material in the transformers are magnetizing materials with ferromagnetic properties. Ferromagnetic materials have high magnetic permeability and hence can be magnetized. Hence the magnetization and demagnetization of the core results in the hysteresis loss as current flows in the forward and reverse directions. Hysteresis loss process is shown in Figure 3.5.

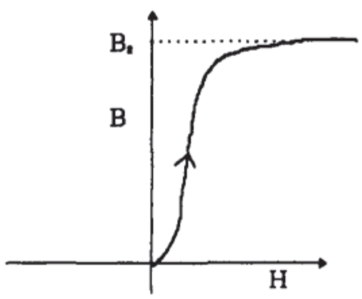

(a)

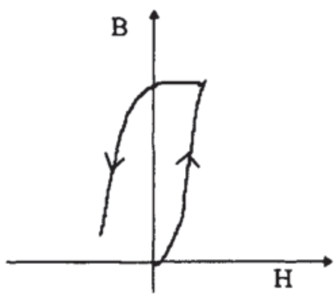

(b)

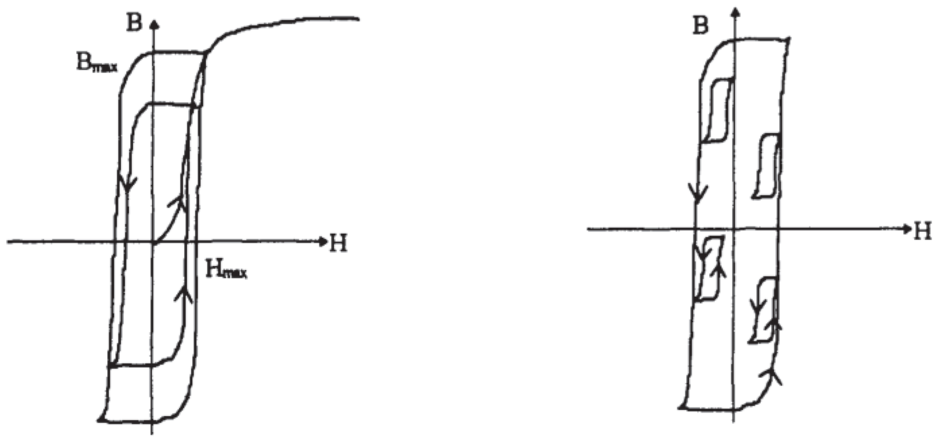

(c) (d)

Figure 3.5. Hysteresis loop process (a) initial curve (b) following a normal hysteresis loop after reversal from the initial curve (c) hysteresis loops (d) minor or incremental hysteresis loops (Del Vecchio et al. 2010)

The hysteresis curve or loop process reflects the relationship between the magnetizing force, H, and the flux density, B. The area of the hysteresis loop shows the energy required to complete a full cycle of magnetizing and de-magnetizing, and the area of the loop represents the energy lost during this process.

The hysteresis loss case is explained as follows: the core material of the transformers are ferromagnetic materials that consist of domains in their inner structure. These domains consist of a number of magnetic dipoles which are parallel with respect to one another inside the domain. Every magnetic dipole in ferromagnetic material has contains unpaired electrons. When these domains are subjected to an external magnetic field, these domains orient in the direction of the magnetic field which gives rise to the net magnetic field. After the magnetic field is removed, most of the domains again orient randomly but some of the domains retain their orientation due to their permanent magnetization. In order to make the magnetic field inside the material zero an external magnetic field should be applied to the opposite direction of the magnetization. Therefore, applied external magnetic field is called as extra work or hysteresis losses to achieve this demagnetization and magnetization of domains.

Another core loss type is eddy current losses which are caused by an alternating current and occurs in the transformer windings due to magnetic fields. The magnetic field will spontaneously cause the eddy currents to flow within the core material. The magnetic core composed of an iron alloy material. The core of the transformer is a good electrical conductor and when an alternating current is applied to the magnetic core, an electromotive force is induced in the material itself according to Faraday's Law of electromagnetic induction principle. This force circulates currents through the core material. These circulating currents are called eddy currents. The power loss caused by these currents is known as eddy current loss.

3.1.3.3. Stray losses

The stray losses are part of the total load loss in the transformer. They are produced by leakage current in the windings, tank, core, core clamping plates, magnetic shields, etc. They include eddy and circulating current loss, loss due to the high current field.

3.1.3.4. Dielectric losses

The dielectric losses play a part in the insulation of the transformer due to the large electric stress. Especially, these losses are occurred in the oil of the transformer, or in the solid insulations, when the oil gets deteriorated or the solid insulation gets damaged, or its quality decreases.

3.1.4. Structure analysis of a dry-type transformer

A schematic view of a 3-phase dry-type transformer is shown in Figure 3.6. As shown in the figure, dry type transformers have no moving parts and is a completely static solid state device that consists of a magnetic core and windings encased in epoxy resin. This makes to these transformers more preferable than oil-filled transformer because the layer of the epoxy resin provides to protect them against fire, dust and corrosion, allows the winding to be flame-retardant, self-extinguishing, and almost maintenance-free. Especially, non-flammable characteristic of these transformers make them suitable for indoor and outdoor applications such as hospitals, underground tunnels, school, steel factories, marines, chemical plants etc. (Azizian and Rahimpour, 2007).

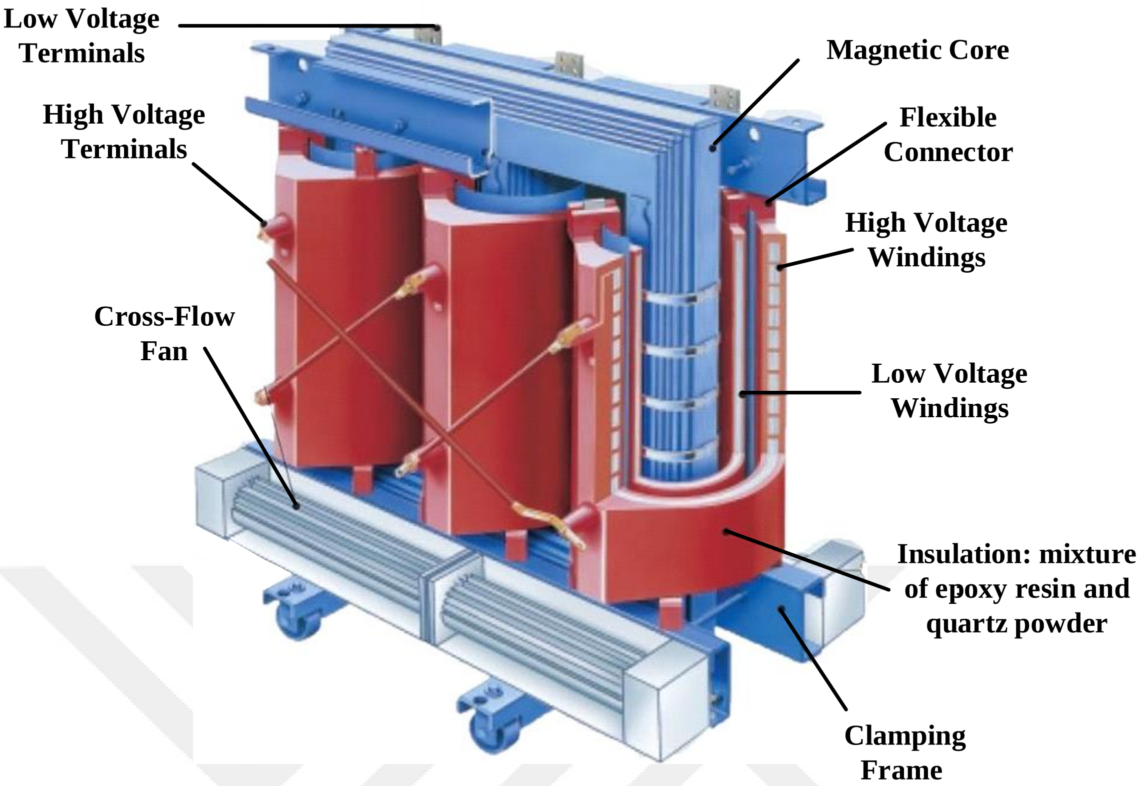

Figure 3.6. A schematic view of a 3-phase dry type transformer.

Moreover, dry type transformers pose no oil leak or pollution risk to the environment. They have a natural cooling mechanism so they require minimal maintenance and eliminating extra cost. When in the condition of natural air cooling, they can be operated long-term continuously under the rated capacity. When the advantages of these transformer are considered, there are several different variations of dry-type transformers used in manufacturing industries. Each of these different types of transformers are manufactured for suitable characteristics and applications.

3.1.5. Types of the dry-type transformers

Dry-type transformers are used in a wide variety of applications and can be installed indoors or outdoors due to their non-flammable characteristic, have better insulation, better dielectric strength, excellent environmental performance, easy installation and maintenance. Thus, there is a variety of types of these transformers made for different purposes.

3.1.5.1. Open-wound transformers

These type of transformers are manufactured with a dip-bake method. In this method, high voltage and low voltage windings of the transformers are pre-heated. Then, the windings are immersed in varnish at an elevated temperature. Finally, the windings are baked to cure the varnish. This method provides to enable higher dielectric strength of the transformers and enhanced protection against fire.

3.1.5.2. Vacuum pressure impregnated (VPI) transformers

These types of transformers have become more popular due to the increasing demand for use of dry-type transformers in moisture-latent or harsh service conditions and chemically-polluted environments. These transformers are designed with high-temperature insulation and additional environmental protection. This protection means that high-temperature materials coated with high-temperature, moisture-resistant and polyester sealants using a vacuum pressure impregnation process. VPI transformers provide excellent mechanical and short circuit strength, no danger of fire or explosion, and no liquids to leak (Nochumson, 2001).

3.1.5.3. Vacuum pressure encapsulated (VPE) transformers

These types of transformers are similar to vacuum pressure impregnated transformers but a small difference is that they are used a silicone resin instead of a polyester resin. Because silicone resin materials have better thermal capability than polyester resins. This thermal capability protects the transformers against the fire during the overload conditions. These transformers were developed for military shipboards due to their non-flammable capability or no danger of explosion, excellent dielectric strength, extended life expectancy, excellent mechanical and short circuit strength (Nunn, 2000).

3.1.5.4. Cast coil resin transformers

One of the main characteristics of cast resin transformers is that the coils of the primary and secondary windings are completely encapsulated in a cast resin body with a smooth surface. Epoxy resin materials prevent penetration of moisture into windings so these materials offer very good protection against adverse ambient conditions. These transformers can work without disruption of service at 100% humidity. Furthermore, compared to the conventional dry-type transformers the cast coil resin transformers are better in respect of impulse voltage withstand strength and have higher dynamic short circuit withstand strength. Due to high-quality insulation material, these types of transformers are practically non-inflammable by an electrical arc, special fire protection measures are not required. When considering the superior features of these transformers, they are the most favorable in various areas such as residential, hospitals, ships and other areas (Azizian, Bigdeli and Faiz, 2016).

3.1.6. Thermal model of a dry-type transformers

In the dry type transformers, iron and copper losses during the conversion of electrical energy cause the temperature increases in the transformer. This temperature increases in the transformers involve the subject of more than one engineering field. For many different types of transformers, many methods such as numerical methods, heat transfer, fluid dynamics, electrical circuit theory, electromagnetic theory can be evaluated together and the transformer heat model can be obtained by using these methods.

In this thesis, the thermal model of the dry-type transformer is based on a computer model, which can predict hot-spot temperatures for different types of cooling regimes and transformer winding geometries coded using ANSYS/Maxwell program. This program uses the Finite Element Method (FEM) that is a numerical method used to solve most engineering problems including stress analysis, heat transfer, electromagnetic distribution and flow of fluids. This method is governed by the following form of the Poisson equation in order to analyze the heat transfer of the 3D dry-type transformer in solid form (Redy and Gartling, 2010).

$$K_x \frac{\partial^2 T}{\partial x^2} + K_y \frac{\partial^2 T}{\partial y^2} + K_z \frac{\partial^2 T}{\partial z^2} = Q \tag{9}$$

or in vector form

$$\nabla.(K\nabla T) = Q \tag{10}$$

where ∇ is the gradient operator

$$\nabla = \hat{e}_x \frac{\partial}{\partial x} + \hat{e}_y \frac{\partial}{\partial y} + \hat{e}_z \frac{\partial}{\partial z} \tag{11}$$

and e_x , e_y and e_z denote the unit vectors directed along the x and y-axes, respectively. T is expressed as the temperature at each point of the considered domain (°C). K (W/m°C) parameters are the thermal conductivities of the transformer in the x, y and z-direction and Q (W/m^3) is the internal heat generation per unit area in the transformer windings and cores. Q is also called as loss density. It is obtained by the losses in the transformer cores (no load losses) and windings (load losses) (Tsili et al., 2012).

3.1.7. Electromagnetic model of a dry-type transformers

Electromagnetic modeling and analysis are the keys structure to find electromagnetic behavior of the transformers with respect to time. This analysis enables to obtain the several electrical characteristics of the transformers or electrical machines like voltages, currents, current density, ohmic loss, core loss, energy and magnetic characteristics like flux lines, field density, field intensity.

In this thesis, electromagnetic analysis of the dry-type transformer is actualized by the ANSYS/Maxwell program. This program is the ability to solve transient, AC electromagnetic, magneto-static, electrostatic, eddy current and electrode transient problems by using Maxwell equations. It provides easy and reliable solution procedures that can give us a more accurate approximation of the desired quantity. ANSYS/Maxwell works on Maxwell's equations which are used for Electro-magnetic analysis.

The appropriate mathematical description of electromagnetic phenomena in a conducting material region is given by Maxwell equations. The equations are based on the Ampere's law, Faraday's law of induction, Gauss' law for magnetism and Gauss' law, respectively, need to be solved in order to obtain a solution of the coupled electromagnetic field (Özupak and Mamiş, 2015). These equations can be expressed as;

$$\nabla x E = -\frac{\partial B}{\partial t} \tag{12}$$

$$\nabla x H = J + \frac{\partial D}{\partial t} \tag{13}$$

$$\nabla . \mathrm{B} = 0 \tag{14}$$

$$\nabla x D = \rho \tag{15}$$

where the field variables are the electric field intensity, E, the magnetic field intensity, H, the magnetic flux density, B, the electric flux (displacement) density, D, the conduction current density, J, and the source charge density, ρ (Redy and Gartling, 2010). Equation 12 is referred to as Faraday's law, Equation 13 express as Ampere's law (as modified by Maxwell), Equation 14 is the as Gauss's magnetic law, and Equation 15 is defined as Gauss's electric law. A continuity condition on the current density is also defined in Equation 16.

$$\nabla . J = \frac{\partial p}{\partial t} \tag{16}$$

This set of equations is solved in ANSYS/Maxwell by means of a magnetic vector potential approach.

3.2. Mathematical Modeling of a 3-phase Dry-Type Transformer

Two major factors are quite significant for the design of all electrical machines. These are efficiency and cost related to weight. Because of this reason, the electrical machines are firstly modeled by using design parameters and then they are optimized in terms of the weight, size and efficiency in order to actualize optimum design. In this section, the mathematical model of a 250 VA 380/110-V wye connected 3-phase dry-type transformer is given in detail. S express the apparent power, U_1 and U_2 are the primary and secondary windings voltages, I_1 and I_2 are the currents flowing through the primary and secondary windings.

$$S = \sqrt{3} x U x I \tag{17}$$

So the currents flowing in the primary and secondary winding are obtained by Equation 17. One of the most significant calculations in the transformer design is the core section. The core section of the transformer (q_{fe}) is obtained by:

$$q_{fe} = C x \sqrt{S_2 x \frac{2}{3}} \tag{18}$$

C parameter is named as the transformer core section acceptability. This parameter varies from 0.7 to 1.5 for 3-phase dry-type transformers. These values depend on the quality of the core. If the quality of the core is good, it gets low value and if it is bad it gets high value. This value directly affects the core section of the transformer (Megep, 2011).

$$0.7 < C < 1.5 \tag{19}$$

Therefore, the first boundary condition or constraint is defined for the optimization of the dry-type transformer.

$$D = \sqrt{\frac{4 x q_{fe}}{0.677 x \pi}} \tag{20}$$

D (cm) is calculated as shown in Equation 20. This parameter is named as the diameter of a leg of the transformer core. Yoke cross-section of the core leg (q_{fej}) should be greater than 20% of the cross-section of the core leg (q_{fe}). This case is inverse for the yoke induction of the core leg (B_j).

$$q_{fej} = q_{fe} x 1.2 \tag{21}$$

$$B_j = \frac{B}{1.2} \tag{22}$$

Total magnetic flux (Φ) passing through the core cross-section is given in Equation 23. This parameter provides to find the primary and secondary windings turn of the transformer.

$$\Phi = Bxq_{fe} \tag{23}$$

It is seen in Equation 24 and 25 that the primary (high voltage) and secondary (low voltage) windings of the transformer are w_1 and w_2.

$$w_1 = \frac{U_1}{\sqrt{3}x4.44xfx\phi} \tag{24}$$

$$w_2 = \frac{U_2}{\sqrt{3}x4.44xfx\phi} \tag{25}$$

HV and LV windings cross-section of the transformer (q_1 and q_2) are presented in Equation 26 and 27.

$$q_1 = \frac{I_1}{s} \tag{26}$$

$$q_2 = \frac{I_2}{s} \tag{27}$$

Where s is the second boundary conditions for the optimization of the transformer. This value is named as the current density of the windings that varies from 2.2 to 3.5 for the 3-phase dry-type transformers. Window height of the core (L_s) is calculated by:

$$L_s = 0.2x\frac{w_1 x I_1}{A_s} \tag{28}$$

A_s denotes the specific ampere winding which is obtained by the characteristic curve shown in Figure 3.7 (Çelebi, 2008).

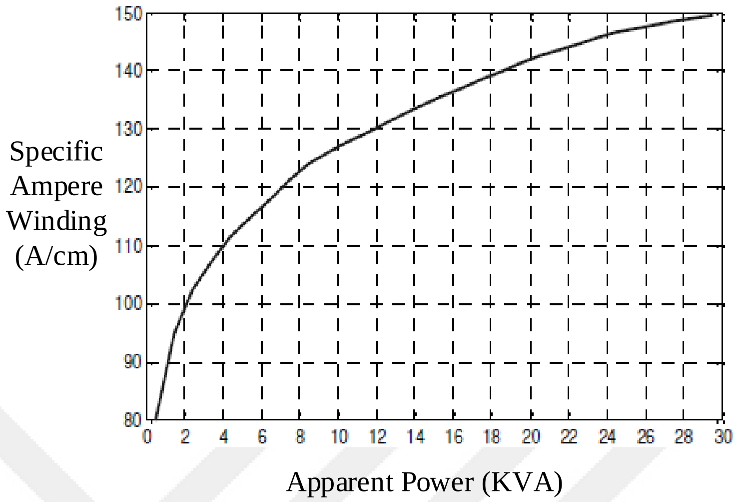

Figure 3.7. The characteristic curve of the specific ampere-winding on dry transformers (Çelebi, 2008).

In equation 29, a is called a window width of the transformer core.

$$a = 4x \frac{w_1 x q_1}{100 x k_{cu} x L_s} \tag{29}$$

k_{cu} represents the window copper filling factor of the transformer core. The characteristic curve of the window copper filling factor is shown in Figure 3.8 (Çelebi, 2008).

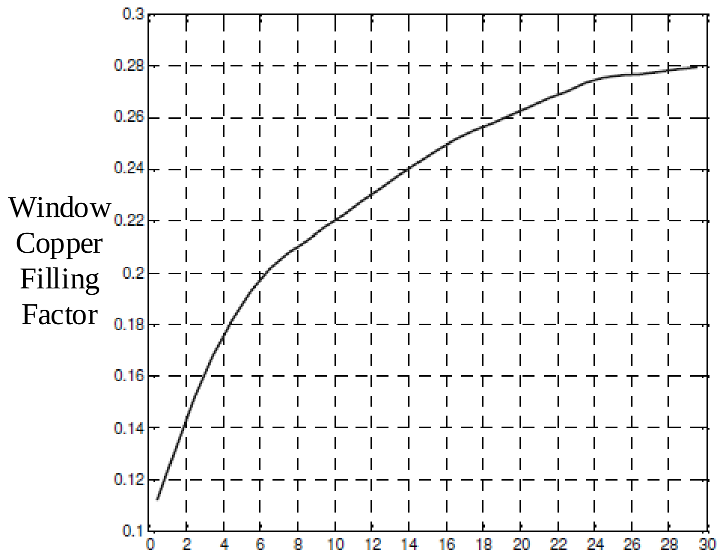

Figure 3.8. The characteristic curve of the window copper filling factor on dry transformers (Çelebi, 2008).

Average lengths of HV and LV windings (l_{m1} and l_{m2}) are used to calculate the copper weight of the windings. a_2 express the radial height of the LV winding.

$$l_{m1} = \pi(\mathrm{D} + 2x0.4 + 0.01x12.2 + 2x1.2) \tag{30}$$

$$l_{m2} = 0.1\pi(10xD + 8 + a_2) \tag{31}$$

The weight of the dry-type transformer consists of the copper weights (windings) and the iron weight (core). The weight of the HV and LV the windings are G_{cu1} and G_{cu2}.

$$G_{cu1} = 3x10^{-5}\gamma_{cu} w_1 q_1 l_{m1} \tag{32}$$

$$G_{cu2} = 3x10^{-3}\gamma_{cu} w_2 q_2 l_{m2} \tag{33}$$

Where, $\gamma_{cu} = 8.9$, denotes the copper-specific weights. Therefore, copper weights of the windings are found for the transformer weight calculation. In order to obtain the winding resistance, resistances of the HV and LV windings are r_1 and r_2 shown in Equation 34 and 35.

$$r_1 = \rho_0 \frac{l_{m1} w_1}{q_1} \tag{34}$$

$$r_2 = \rho_0 \frac{l_{m2} w_2}{q_2} \tag{35}$$

The winding resistances, primary and secondary currents of the transformers are known so copper losses of the transformer (P_{cu1} and P_{cu2}) are obtained easily.

$$P_{cu1} = 3 I_1^{\ 2} r_1 \tag{36}$$

$$P_{cu2} = 3 I_2^{\ 2} r_2 k \tag{37}$$

k denotes the resistance increase factor due to the current accumulation of the windings. Therefore the total copper losses of the transformer are P_{cu}.

$$P_{cu} = P_{cu1} + P_{cu2} \tag{38}$$

Core losses are the other losses of the transformer. These losses are the iron loss for each of the three legs (P_{feb}) and iron loss for the yoke (P_{fej}). Firstly, the iron weights must be calculated to obtain the core losses. The weight of 3 legs of the transformer core (G_{feb}) is expressed as follows.

$$G_{feb} = 3x10^{-3}\gamma_{fe}q_{fe}L_s \quad (39)$$

γ_{fe} denotes the iron specific weight constant. This value is a constant selected to 7.6 (Çelebi, 2008). Another weight parameter is G_{fej} called as the weight of the transformer yoke. This parameter is expressed where $M = 0.851xD + 0.1xL_s$.

$$G_{fej} = 3x10^{-3}x\gamma_{fe}xq_{fej}x2x(0.8x\,\mathrm{M} + 0.8x\,\mathrm{D}) \quad (40)$$

Specific yoke and leg iron loss in the transformer core are p_{fej} and p_{fe} expressed as follows.

$$p_{fej} = p_{10}x\xi_2 xB_j^{\ 2} \quad (41)$$

$$p_{feb} = p_{10}x\xi_2 xB^{\ 2} \quad (42)$$

ξ_2 denotes as the loss factor during the core process and p_{10} express the additional loss factor of the core. The yoke (P_{fej}) and 3-leg iron loss (P_{feb}) in the transformer core are easily calculated by using the previous equations.

$$P_{fej} = G_{fej}xp_{fej} \quad (43)$$

$$P_{feb} = G_{feb}xp_{feb} \quad (44)$$

Hence, the total iron losses in the transformer core are expressed as Equation 45.

$$P_{fe} = P_{feb} + P_{fej} \tag{45}$$

The total weight (G_{total}) of the 3-phase dry-type transformer is equal to the total amount of the HV coils weight, the LV coils weight, the yoke weight of the core, and the 3-leg weight of the core, and it is given in Equation 46:

$$G_{total} = G_{cu1} + G_{cu2} + G_{feb} + G_{fej} \tag{46}$$

The copper and core losses of the transformer create the total loss of the transformer shown in Equation 47.

$$P_{total\_loss} = P_{cu} + P_{fe} \tag{47}$$

The efficiency of the transformer (η) is found by dividing the output power to the total losses and output power of the transformer.

$$\eta = \frac{S_2}{S_2 + P_{total\_loss}} \tag{48}$$

As a result, upon taking consideration into account of the mathematical model of the transformer, the constraints, efficiency and weight functions of the transformer are obtained for the optimization process of the transformer. The constraints are current density parameter (s) and the transformer core quality factor (C). These values have a significant role in the transformer design and optimization. The weight, size and efficiency of the transformer are directly related to these constraints since they are the key parameters on the transformer losses, core and windings weights.

3.3. Particle Swarm Optimization

Optimization is a scientific method interested in the determination of the best-suited solution for a problem, among alternatives. The major aim of the optimization is to minimize the problem required or to maximize the desired benefit. Optimization problems may be linear or non-linear. Therefore, optimization methods must have specialization of algorithms to different problem categories such as nonlinearity, convexity, differentiability, continuity, function evaluation accuracy etc. because of the different nature and mathematical characteristics of them. The particle swarm optimization (PSO) is a heuristic global optimization method that shown the effective in optimizing difficult multidimensional discontinuous problems in a variety of fields.

Particle Swarm Optimization is an optimization algorithm developed by Kennedy and Eberhart in 1995, inspired by observing that the movements of some animals moving in swarm while the animals meeting their basic needs such as finding food affect other individuals in the swarm and that the swarm can achieve its purpose more easily (Kennedy and Eberhart, 1995). In PSO, each individual searching for a solution is called a particle, while the population of particles is called a swarm. The fitness function is used to understand how close an individual is to a solution. The main purpose of this function is to measure how close we are to the real solution. Each particle adjusts its position to the best position in the swarm, using its previous experience. Other particles update their movements according to the individual who has the best position of the swarm at that moment. This movement velocity is a phenomenon that develops at random, and in general, the particles are in a better position in their new movement than in the previous one. This process continues until the swarm reaches the target. The best state in which a particle approaches the solution during its search for a solution is called personal best (pbest). In the whole swarm, the current state of the particle most closely approaching the solution during the entire search is called global best (gbest). The PSO method involves, at each iteration, changing the velocity (accelerating) each particle toward its pbest and gbest locations (global version of PSO) (Eberthart and Shi, 2001).

In PSO, firstly the swarm to search for the solution and the necessary parameters are determined. The proximity to the solution of the particles is measured with the help of the fitness function and the pbest and gbest values are updated according to these values.

Then, the changing velocity function is used to determine the movement of each particle and set new states. The fitness function is used again to check how close the solution. This cycle is repeated until the desired conditions are reached. The cycle is shown in Figure 3.9.

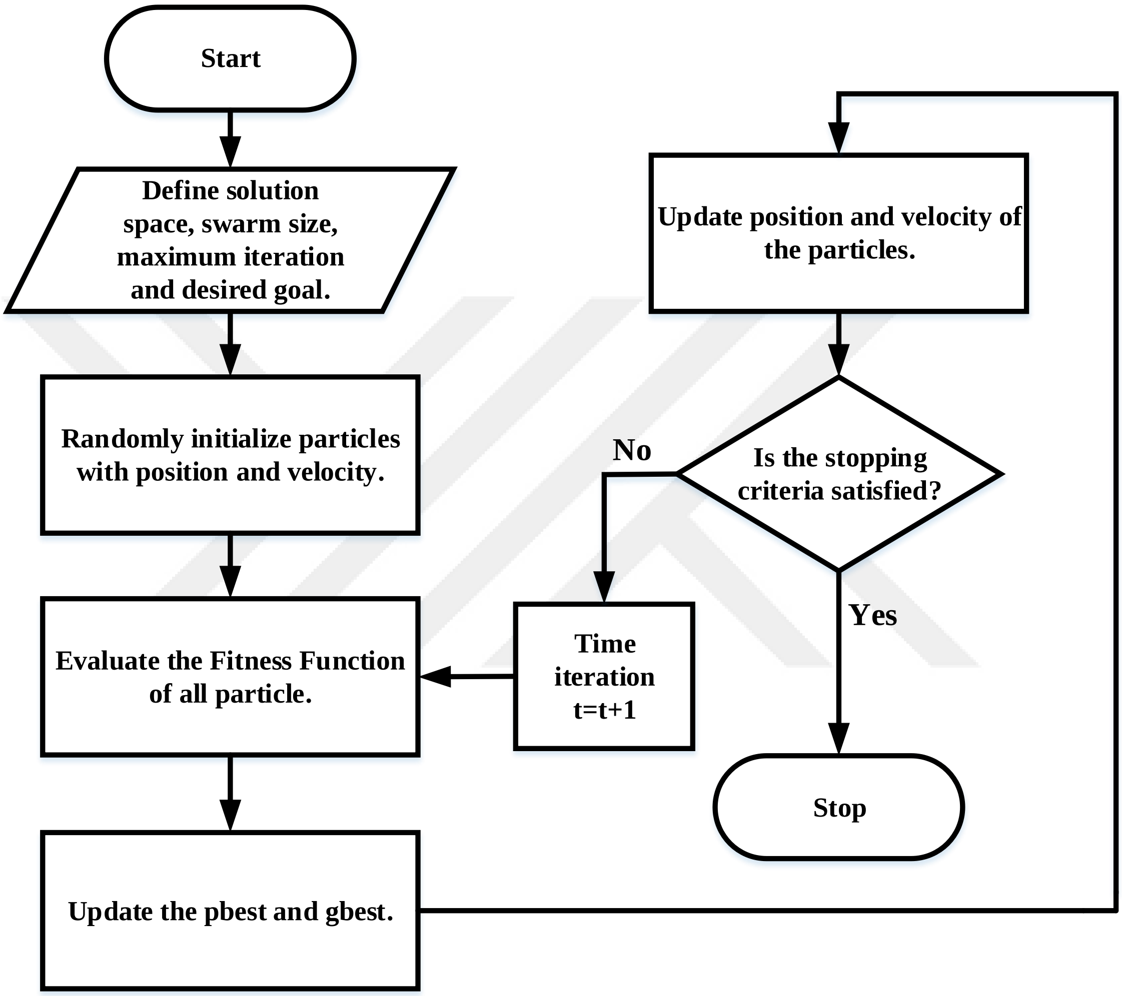

Figure 3.9. The standard flowchart of the PSO algorithm (Kalatehjari, Hajihassani and Ali, 2014).

In PSO, the swarm starts with an initial solution. Initially, each particle has a speed and position value. Particle positions are variable values within the defined range. The particles move by adjusting their speed according to both themselves and the swarm. The particles approach a little closer to the optimum solution at each iteration. The velocity and position formulas of the particle are as given in Equations 49 and 50.

$$v_i^{n+1} = y(v_i^n + c_1 \, \mathrm{rand}_1 (\mathrm{p}_{best\,i}{}^n - \mathrm{x}_i^n) + c_2 \, \mathrm{rand}_2 (\mathrm{g}_{best} - \mathrm{x}_i^n)) \tag{49}$$

In this equation, n is the number of iterations. x is called as the particle value. v_i^n is the velocity of the ith particle in the nth iteration. v_i^{n+1} express the speed for the next iteration. y, c_1 and c_2 are interconnected coefficients. The y restriction factor has the effect of damping oscillation in the motion of the particles. Therefore, the particles approach the result over time. c_1 and c_2 are social and cognitive parameters. A rand is a number (0-1) randomly drawn from a uniform random distribution. Once the speed is calculated, the position is calculated with the following formula.

$$x_i^{n+1} = x_i^n + v_i^{n+1} \tag{50}$$

K is a constant connected to c_1 and c_2. In equation 51, the formula of y constant is given.

$$K = \frac{2}{\left|2 - c - \sqrt{c^2 - 4c}\right|} \;,\; c = c_1 + c_2 \,,\; c > 4 \tag{51}$$

c_1 allows the particle to move according to its own experience (cognitive), and c_2 allows it to move according to the experience of other particles in the swarm (social). In PSO, the particle number can be between 20 and 40. The number of particles can be increased if more accurate measurements are required. Problem number of variables and the value range of the variables vary according to the problem. c_1 and c_2 are usually selected close to 2. If the values 2 and 2.1 are taken respectively, the y constant is used as 0.7298 (Erdoğmuş and Yalçin, 2015).

3.3.1. PSO algorithm parameters

To understand the conceptual basis of the PSO is necessary to know the algorithm parameters needed to implement the optimization. PSO algorithm consists of some basic parameters which have a large impact on its efficiency performance. These parameters are the swarm size (number of particles in the swarm), iteration numbers, velocity components and acceleration coefficients. The parameters are given in detail the following sections.

3.3.1.1. Swarm size

The number of particles in the swarm is expressed as swarm size or population size in PSO. If there are many particles in the swarm, the initial diversity of the swarm is greater provided that a good uniform initialization scheme is used to initialize the particles. A huge swarm creates larger areas of the search space in every iteration. A large number of particles may increase the per iteration computational complexity and also cause more time-consuming. On the contrary, a huge swarm may enable fewer iterations in order to obtain optimal results or best solutions. The algorithm is capable of reach good solutions with small swarm sizes of 10 to 30 particles. (Talukder, 2011). However, an optimal result has even been obtained for fewer than 10 particles (Van denBergh, 2002).

3.3.1.2. Iteration numbers

In order to acquire an optimal solution, iteration numbers are also dependent on the problems. If the iteration numbers are too low, this case may cause terminating the search prematurely. On the other hand, a too large number of iterations may result in computational complexity and more time consuming (Engelbrecht, 2007).

3.3.1.3. Velocity components

One of the most important factors is the velocity components because they provide to update the particle’s velocity. Velocity components consist of three terms: previous velocity, cognitive velocity and social velocity.

Previous velocity (v_i^n) is also named as inertia component that serves a memory of the previous flight direction. That is stated as the movement in the immediate past. While the memory term is expressed as a momentum prevents to considerably change the direction of the particles and to bias towards the current direction.

Cognitive velocity ($c_1 \text{rand}_1(\text{p}_{best\,i}{}^n - \text{x}_i^n)$) evaluates the particle productivity according to past performances. In one way, it seems a singular memory of the position that was optimal for the particle. Kennedy and Eberhart qualify the cognitive component as the "nostalgia" of the particle (Kennedy and Eberhart, 1995). The major impact of the cognitive component is that particles represent the tendency of individuals to return to the most satisfactory positions in the past.

Social velocity ($c_2 \text{rand}_2(\text{g}_{best} - \text{x}_i^n)$) evaluates the performance of the particles as to a group of particles or neighbors. The major impact of the social velocity is that every particle tends to the optimal position found by the particle's neighborhood.

The geometrical illustration of the velocity components' velocity and position updates are shown in Figure 3.10.

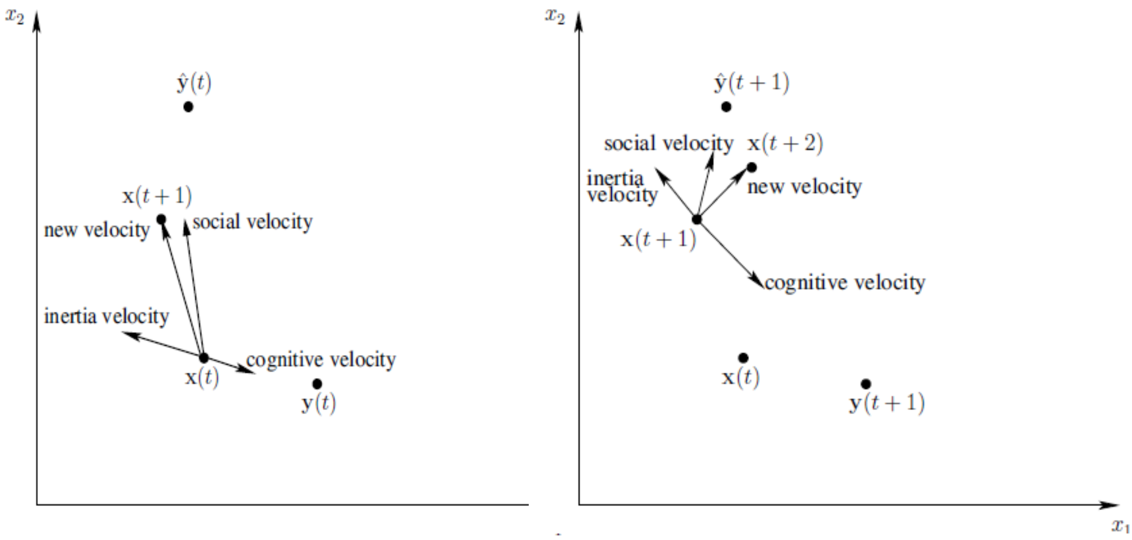

(a) (b)

Figure 3.10. Geometric illustration of a particle's movement in PSO for a single two-dimensional particle (a) iteration time = t (b) iteration time = t+1 (Tokhi and Alam, 2010).

3.3.1.4. Acceleration components

The acceleration components are termed as c_1 and c_2 which provide to maintain the stochastic effect of the cognitive and social components of the particle's velocity respectively. This component works with the random values coordinately. c_1 states the measurement of the reliance of a particle in itself. While c_2 states the measurement of the reliance of a particle in its neighbors.

- If the c_1 = c_2 =0, each particle maintain their current speed until they reach the boundary area of the search space. Thus, the velocity update equation is as follow.

$$v_i^{n+1} = y(v_i^n) \tag{51}$$

- If the c_1 > 0 and c_2 = 0, each particle, the velocity components are the independents. The velocity update equation is shown in Equation 52.

$$v_i^{n+1} = y(v_i^n + c_1 \mathrm{rand}_1(\mathrm{p}_{best\,i}{}^n - \mathrm{x}_i^n)) \tag{52}$$

- If the c_2 > 0 and c_1 = 0, each particle moves to a single point in the swarm. This phenomenon is called as g_{best}. Therefore, the velocity update equation will become

$$v_i^{n+1} = y(v_i^n + c_2 \mathrm{rand}_2(\mathrm{g}_{best} - \mathrm{x}_i^n)) \tag{53}$$

- If the c_2 = c_1, each particle moves towards the average of $\mathrm{p}_{best\,i}{}^n$ and g_{best}.
- If the c_1 >> c_2, each particle is strongly effected by its p_{best} position. On contrary, if c_2 >> c_1, this case results in that each particle is much more influenced by g_{best} position.

3.3.2. Advantages and disadvantages of PSO

It is said that PSO is a swarm based stochastic optimization method for solving the non-linear global optimization problems. This optimization method has many superior features while there are disadvantages of the PSO algorithm. The negative and positive features (advantages and disadvantages) of the PSO method are discussed below table.

Table 3.1. Advantages and disadvantages of Particle Swarm Optimization (PSO) (Abdmouleh et al., 2017).

Advantages	• The algorithm is a derivative-free algorithm. • It is easily implemented for solving problems, thus it is performed both in scientific research and engineering problems. • It has short computational time and also is the capability to run the parallel computation. • It needs a limited number of parameters and the effect of parameters in order to the problem solutions is more effective compared to other optimization techniques. • It is suitable for solving problems presenting difficulty to reach accurate mathematical models. • It has a higher probability and impact in finding the global optimum results.
Disadvantages	• It can be hard to determine initial design parameters. • It has a lack of' the regulation of speed and direction.

3.4. ANSYS/Maxwell Program

ANSYS is an analysis software that is widely used in industry and provides numerical analysis of problems. It is a computer-aided engineering program that uses finite element analysis (FEA) method to solve electric or magnetic problems. FEA was first developed in 1956 for the stress analysis of airframes, and then it was used in the solution of applied sciences and engineering problems in the following decade (Fish and Belytschko, 2007). In the following years, these methods and solution techniques have been developed rapidly and have become one of the best methods for solving many engineering problems. The basic logic in FEA is to simplify and solve a complex problem. In this method, the solution region is divided into a plurality of simple, small, interconnected sub-regions called finite elements. In other words, the problem which is divided into parts connected by a plurality of nodes can be easily solved. The working principle of the FEA method is explained as follow.

- The structure is fragmented. (With elements containing nodes)

- Define the behavior of physical quantities for each element. (With elements containing nodes).

- By connecting the elements from the joints, an approximate system of equations is created for the whole structure.

- System equations are solved for unknown values in the joints. (For example, relocation).

- The desired values of the selected elements are calculated. (For example stresses).

FEA method has found its place in many fields today. In addition to structural mechanical problems, this method is used to solve engineering problems related to heat conduction, fluid mechanics, electrical and magnetic fields. One of the reasons why the method finds so many applications is the similarities between different engineering problems. Some of these fields in the wide range of finite element method can be listed as follows:

- Machinery / Aircraft / Construction / Automotive Engineering Applications.

- Structural Analysis (Static, Dynamic, Linear / Nonlinear).

- Thermal, Flow Calculations,

- Electromagnetic Calculations,

- Biomechanical Calculations,

- Medical Applications and so on.

With the advancement of technology, the increase in inventions complicated by the use of finite elements in solution systematics has increased. This very useful method has been integrated into many analysis programs and found its place in different fields of use.

ANSYS/Maxwell solves the electromagnetic field problems by solving Maxwell's equations in a finite region of space with Appropriate boundary conditions and when necessary with user-specified İnitial conditions in order to obtain a solution with guaranteed uniqueness. This program consists of many solution types in order to analyze a non-linear geometry both in electromagnetically and thermally. These types of solutions are the magneto-static, eddy current, electrostatic and transient solutions. Static magnetic fields, forces, torques, and inductances caused by DC currents, static external magnetic fields, and permanent magnets. In this case, the magneto-static solution type is suitable for linear or nonlinear materials. Eddy current solver is effective for sinusoidally-varying magnetic fields, forces, torques, and impedances caused by AC currents and oscillating external magnetic fields. This solver type is only used for linear materials. The electrostatic solver is suitable for static electric fields, forces, torques, and capacitances caused by voltage distributions and charges. This solver type is also used for linear materials only. The transient solver is effective for transient electric / magnetic fields caused by time-varying voltages, current (AC / DC) or current excitations. This solver type is used for both inhomogeneous and nonlinear materials. Depending on the choice of the solver in the program, the solution is realized by using appropriate equation sets and terms.

ANSYSMaxwell has three different design types. These are RMxprt, Maxwell 2D and Maxwell 3D. Rmxprt (Rotation Machinery Expert) is used in the design and analysis of electrical machines. Maxwell 2D performs finite element method analysis using XY or RZ planes, while Maxwell 3D performs finite element method analysis using three-dimensional electromagnetic field solutions. In this thesis, Maxwell 3D is used to analyze the designed transformer model electromagnetically. In Maxwell 3D, the basic unit of the finite element is tetrahedron. All of the tetrahedral structures in the model are called simply mesh or finite element mesh of the whole model. The assembly of all tetrahedral structures is referred to as the finite element mesh of the model or simply the mesh. In ANSYS/Maxwell, the meshing process is very important because the accuracy of the calculated results is directly influenced by the meshing process. Maxwell automatically processes all objects (models) before the analysis process begins. Users can make changes about how to do mesh operation in the program. Realization of the analysis flow diagram of a model by using Maxwell 3D is shown in Figure 1.

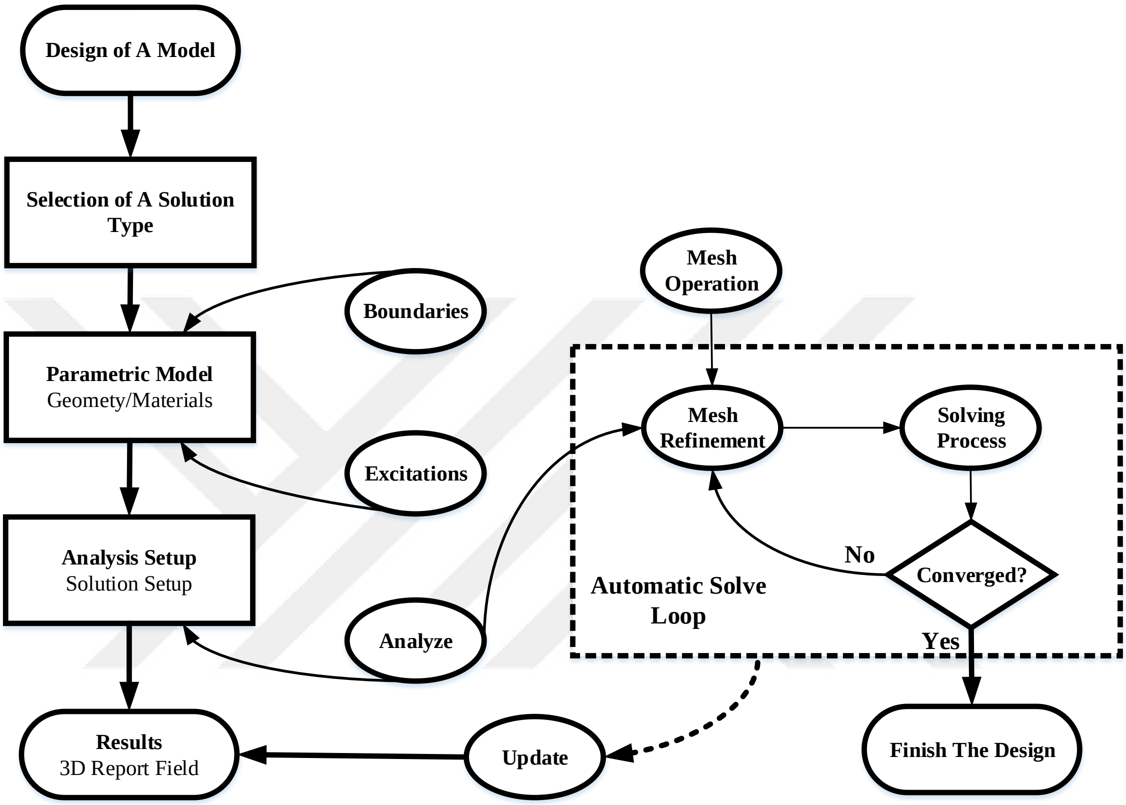

Figure 3.11. Analysis flow diagram of a model in Maxwell 3D.

3.5. PLC (Programmable Logic Controller) Measurement Station

PLC (Programmable Logical Controller) is an automation device which is used to control processes such as control of machines in production departments or factories. Unlike normal computers, the PLC has several inputs and outputs (I / O). One of the most significant advantages is designed to withstand electrical noise, temperature differences and mechanical impacts. PLCs of different brands uses an operating system of their own. This supervisory system scans the input information at invisible speeds and works to respond to the corresponding output information in real time. PLC plays a major role in the production of more and better quality products in a short time and production with very low error rates. The most important feature of the PLC is that the given program commands are processed in real-time, and the functions are transmitted to the external world-related modules such as input/output and communication as soon as possible. Thus, they can be used in industrial applications where timing is critical.

PLCs include components such as a central processing unit (CPU), RAM and ROM memory, input/output module, communication modules required for storing and running programs. The CPU is the most important unit that regulates the operation of the PLC, performs all arithmetic and logical operations, and performs tasks such as timing and counting. The part that gives intelligence to PLC is CPU and memory. Two separate PLCs can use the same microprocessor. However, the functions of the PLCs may also be different since the operating systems are different. The memory unit is divided into sections such as input image, data, program memory. Each memory area has different functions. In PLCs, generally, EPROM (Erasable Programmable Read Only Memory) is used as a memory element. This memory space, as the name implies, means erasable, rewritable, programmable, read-only memory. Each PLC has its own program and these programs are stored in the PLC's memory. It is also sent from memory to the central processing unit. The input module is expressed as a unit that converts analog signals from the sensing elements of the controlled system into logical voltage levels that the PLC understands. Depending on the type of sensor in the controlled system, binary values (1 or 0) from elements such as pressure, level, temperature, control, proximity are received via the input unit. Input voltage values can be 24V, 48V, 100V-120V, 200V and 240V direct or alternating current. The output unit is the unit that converts the logic voltage for the output points calculated in the PLC into electrical signals suitable for driving control elements such as contactors, relays, the solenoid in the controlled system. The output unit may consist of relay, triac or transistor circuits. PLCs are also usually used with relay output units. However, transistor or triac output units are used in cases where high speed opening and closing is required. Communication module enables to a data connection between the CPU and Human Machine Interface (HMI) or computer. The operating mechanism of these components is shown in Figure 3.12.

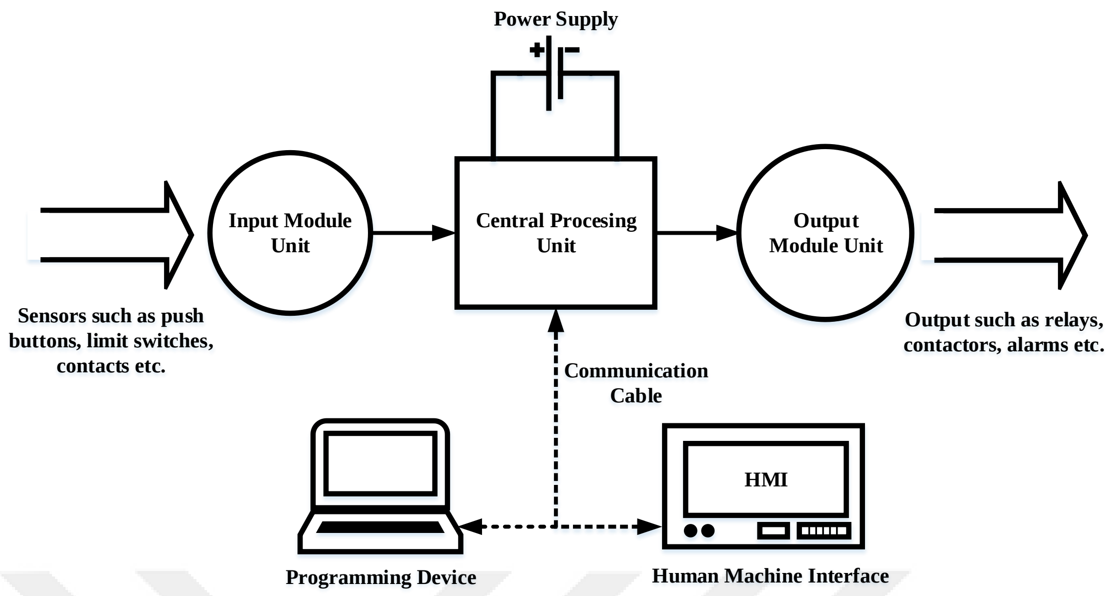

Figure 3.12. Operation mechanism of PLC with its basic components.

For this thesis, PLC measurement station is created and designed for analyzing temperature rises in the transformer. It provides to observe the temperature distribution on the transformer. In order to obtain accurate results, the effective and high degree of accuracy PLC equipment is used. The thermal measurements are taken from 6 different points of the transformer by using PLC measurement station. The transformer core, primary and secondary windings of the transformer are measured at load and overload condition. The designed PLC measurement station consists of basically a CPU, analog modules, HMI panel, communication cable, DC power supply and thermocouples. FATEK FBs-20MAR series CPU is used in this station. FATEK FBS Series PLC is a new generation of micro PLCs with its advanced product functions and its ability to expand to five communication ports. The maximum number of digital I/O is 512, with 64 analog inputs and 64 analog outputs. Table 3.2 shows detailed information about the used CPU unit.

Table 3.2. Technical specifications of the CPU unit (FBs-20MAR).

Characteristics			FBs-20MAR
Digital Input	24V DC	Medium Speed (20 kHz)	4 Pieces
Digital Output	Relay		8 Pieces
Communication Port	Settled		1 port (Port0, USB or RS232)
	Extension		2 port (Port1~2, RS485, RS232 or Ethernet)
Real Time Clock	Optional		
Built-in Power Supply	SPW14-AC/D12/D24		
Connection Type	7.62mm terminal block		

Another equipment in part of PLC measurement station is the analog input module (FBs-6AD). It is one of the analog input modules of FATEK FBs series PLC. It provides 6 channels A/D input with 12 or 14 bits effective resolution. Base on the different jumper settings it can measure the varieties of current or voltage signal. The reading value is represented by a 14-bit value no matter the effective resolution is set to 12 or 14 bits. In order to filter out the field noise imposed on the signal, it also provides the average of the sample input function. I/O addressing of FBs-6AD inputs starts from the module closest to the main unit, respectively CH0-CH5 (1st module), CH6-CH11 (2nd module), CH12-CH17 (3rd module) and so on. For each module, the sample is added 6 at a time, and in total is 64 (from CH0 to CH63), and is compatible with the reciprocal internal analog registers of the PLC. 6 different measurement sensor are simultaneously used thanks to the selected analog input module. The main procedure of using this module is summarized in Figure 3.13.

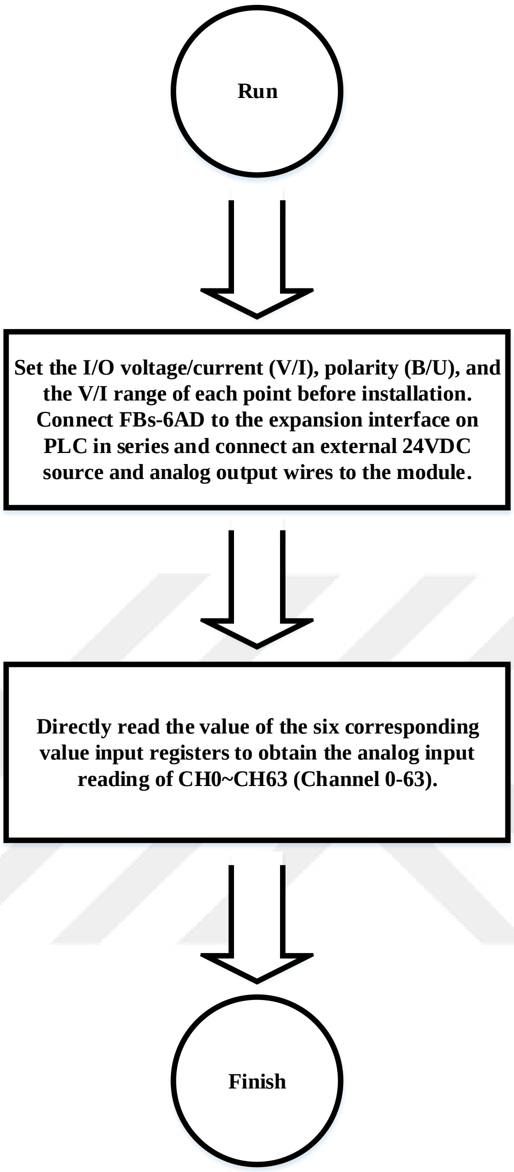

Figure 3.13. Operation mechanism of PLC with its basic components.

Finally, thermocouples (Type-J) are used to measure the temperature rise in the transformer. The thermocouple is a simple temperature measuring element which is formed by welding the ends of two different alloys. The weld point is referred to as a hot spot, and the other two open ends are referred to as a cold point (or reference point). The thermocouple event arises from the temperature difference between the hot spot and the cold spot. A voltage of mV is generated at the cold point ends proportional to this temperature difference. Regardless of the temperature distribution between the hot point and the cold point of the thermocouple, the generated voltage is proportional to the temperature difference between the hot point and the cold point. Thermocouples (thermocouples) are used in a wide range of applications in temperature measurement in industry. Although the thermocouple is actually two different metal or alloy wires, they are generally not directly immersed in the process. Various mechanical impacts, physical and chemical abrasive properties are taken into account in certain special protective sheaths are used. Since two different element wires are at different poles, they are isolated from each other with the help of insulators. In the selection of the isolators, again the environmental conditions and the temperature limits are very important. Both the element wires and the protective tubes have a direct effect on the life of the thermocouples.

J-type thermocouples are suitable and durable to measure higher temperature accurately. In J Type Thermocouple mainly magnesium oxide (MgO) insulation is used. Due to many desirable characteristics of MgO such as fast response, compact size, broad temperature range, formability, weld ability, durability, accuracy, thermal shock and vibration resistance makes it an excellent choice for virtually all laboratory or process applications. The standard average temperature increase for dry-type transformers of the standard class is 80,115 and 150 degrees, while the hottest spot temperature is a maximum of 150,185 and 220 ° C, respectively (ANSI/IEEE C57.94™-1982, 2006). Therefore, the temperature range of thermocouples is selected by considering of IEEE standards. J-type thermocouple characteristic table is shown in Table 3.3.

Table 3.3. The characteristic table of the J-type thermocouple.

Characteristics	**J-Type Thermocouple**
Maximum operating temperature	-200°C …800°C
Standard cable types	Standard Production: Glass fiber + glass fiber + steel mesh, 2x 0,22mm (Silicone + Silicone, 2x 0,22mm: “Si + Si” can be added to the order code)
Standard cable lengths	K01 = 1 mt, K1.5 = 1.5 mt, K02 = 2 mt K03 = 3 mt, K04 = 4 mt, K05 = 5 mt
Sensor type	DIN/IEC-584 “J” FeCu-Ni E= J,
The material of protective sheath	Nickel-plated brass

Connector (Screw Size)	1/4 x 19” (can be produced as optional M12)
Sensor Diameter	6 mm
Accuracy	±1.1°C or 0.4%

Temperature measurements are taken from J-Type thermocouples using PLC measuring station. Temperature analog data is received with the help of these thermocouples and sent to the corresponding addresses in the analog input modules. The obtained data in the CPU which is communicated with the analog input modules are processed. Current data between the 4 ma and 20ma are received from the sensors. The data is scaled according to the minimum and maximum values of the sensors. The current rates of the software in the CPU are converted to the operating rates of the sensors and output is obtained. These output values are recorded with the software in the CPU and sent to the Excel file and saved to the Excel file according to the desired time intervals. Thanks to the PLC measuring station, data can be read instantly via the HMI panel. The temperature measurement and recording process are summarized in Figure 3.14.

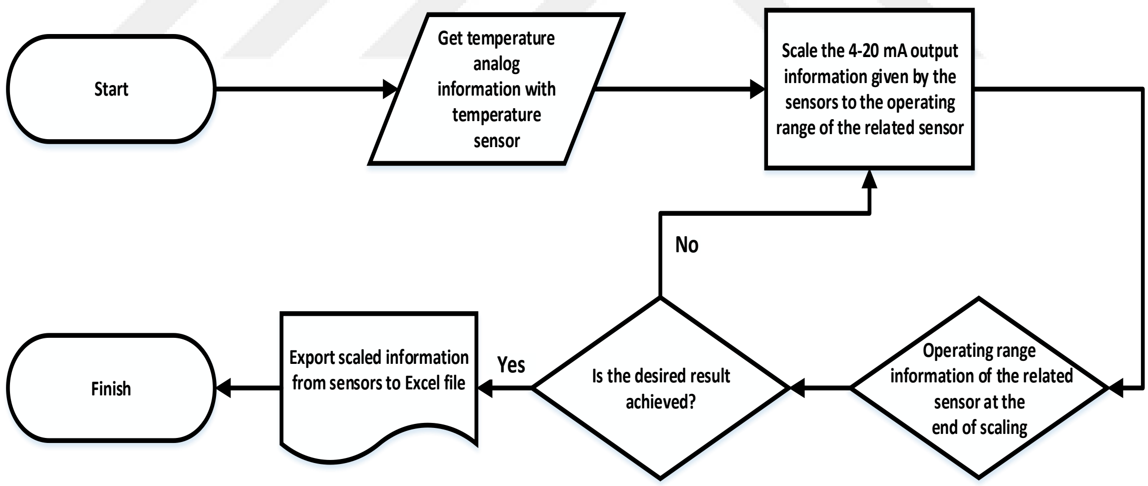

Figure 3.14. Flowchart of the temperature measurement process by using thermocouples.

Designed PLC measurement station in order to measure, observe and record the temperature data is shown in Figure 3.15.

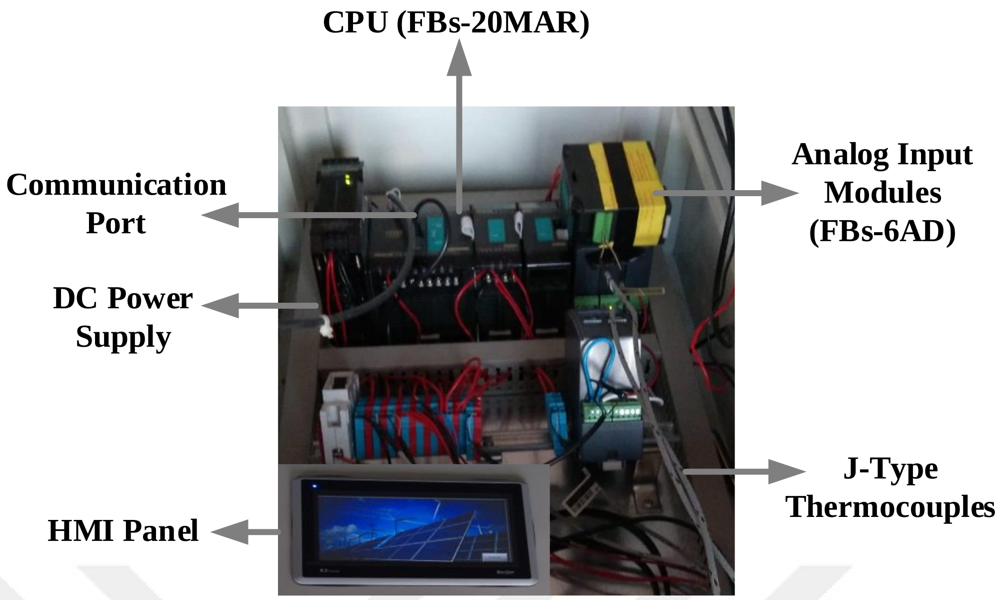

Figure 3.15. Designed PLC measurement station for the 3-phase dry-type transformer.

4. RESULTS AND DISCUSSIONS

A 250 VA 380/110-V wye connected 3-phase dry-type transformer are analyzed both in electromagnetically and thermally at the laboratory conditions. Firstly, the transformer parameters are obtained by using a mathematical model of the 3-phase dry-type transformer referred in section 3.2. These parameters consist of transformer losses (such as copper losses, core losses and stray losses), the weight of the transformer (such as core weight, the primary and secondary winding weight that is also include resin) and the core and windings dimensions of the transformer. After the parameters are obtained by using this classical mathematical model of the 3-phase dry-type transformer, these parameters are optimized in terms of the weight and efficiency thanks to Particle Swarm Optimization (PSO) method. In order to realize the PSO optimization, core quality factor (C) and current density of the windings (s) are used as the boundary conditions of the transformer. The transformer is re-designed and manufactured efficiently and cost-effectively by using the optimized parameters.

After the optimization process, this transformer is drawn in ANSYS/Maxwell program. This program is suitable for design and electromagnetic/thermal analysis applications of the electrical machines. The design steps of the transformer core and windings will be performed in detail. Finally, the designed transformer is analyzed in the laboratory. This transformer is tested at the load and overload conditions in order to observe the temperature rises in the transformer. AC voltage and current measurements of the transformer primary and secondary windings are provided by the power analyzer (Unit UT 267B). The temperature measurements are obtained and recorded via the PLC measurement stations. In addition, temperature distribution on the transformer core and windings are observed thanks to thermal imaging camera. This camera also provides to observe the critical temperature points of the measured transformer in detail. Time-dependent changes in electrical currents and voltages are monitored in real time with the help of oscilloscope.

As a result of the simulation and test studies, the studies are compared with each other to verify the accuracy of the results. Figure 4.1 shows the modeling and realization of the transformer with optimum weight and efficiency characteristics step by step. All steps will be represented in the following sections.

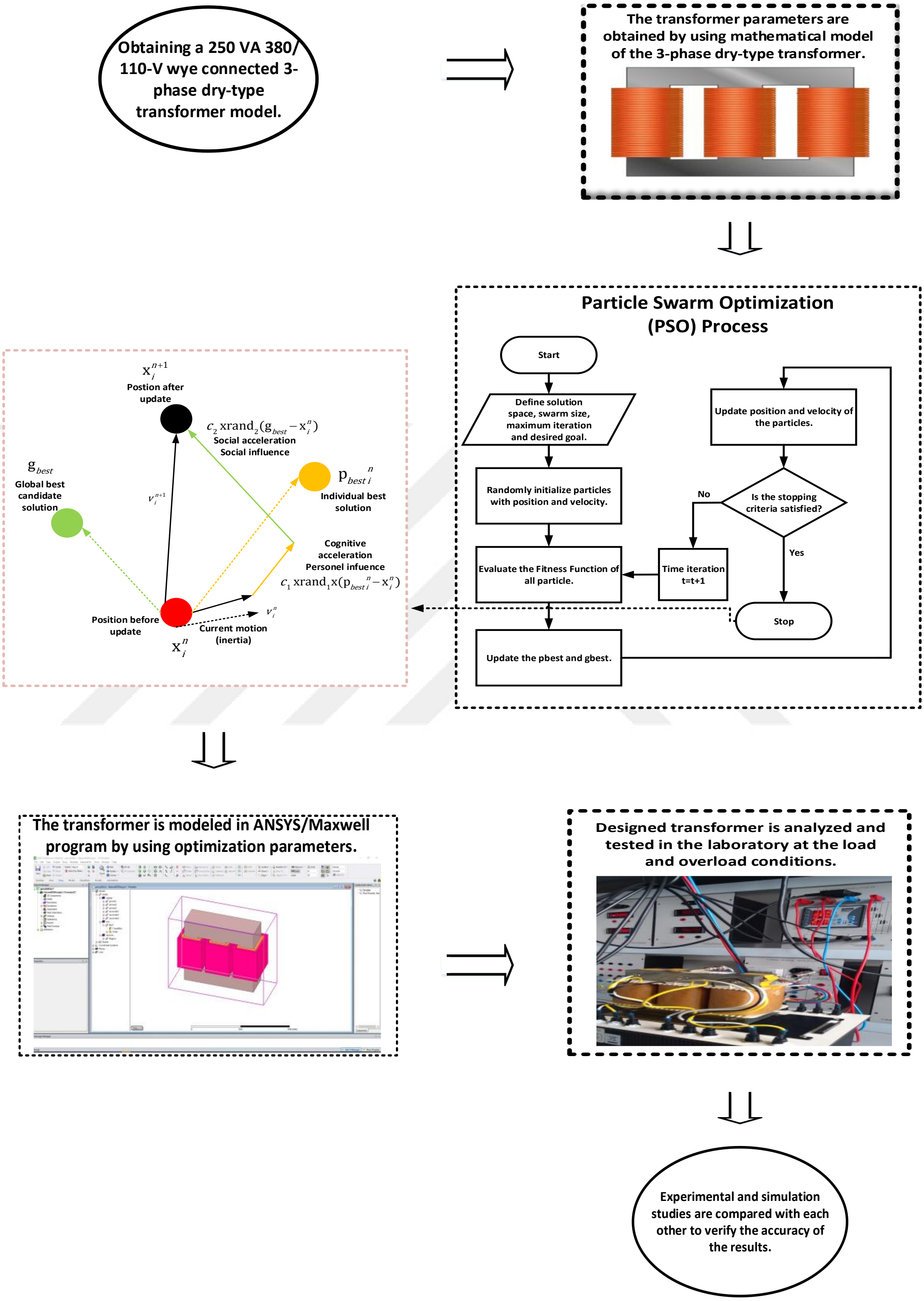

Figure 4.1. Steps for modeling and realization of the transformer with optimum weight and efficiency characteristics.

4.1. Parameters of the analyzed 3-phase dry-type transformer

The parameters of a 250 VA 380/110 V dry-type transformer is obtained by the mathematical model of the transformer. Table 4.1 presents the weight, electrical and electromagnetic parameters of the transformer in detail.

Table 4.1. A 250 VA 380/110 V 3-phase dry-type transformer design parameters obtained by using a mathematical model of the transformer.

Symbols	Parameters	Units	Values
S_2	Secondary Apparent Power	VA	250
$U_{1\phi}$	Primary Phase Voltage	V	220
$U_{2\phi}$	Secondary Phase Voltage	V	63.5
q_{fe}	Core section of the transformer	cm^2	13.29
s	Current density	A/cm^2	2.2
C	Transformer core section acceptability	-	1.03
∅	Magnetic Flux	Weber	0.0018
w_1	Primary Windings	turns	320
w_2	Secondary Windings	turns	95
I_1	Primary Current	A	0.4
I_2	Secondary Current	A	1.31
D	Diameter of a leg of transformer core	cm	5
q_1	Primary Winding Cross Section	mm^2	0.2
q_2	Secondary Winding Cross Section	mm^2	0.6
L_s	Window height of the core	cm	6.8
a	Window width of the transformer core	cm	3
l_{m1}	Average lengths of HV winding	cm	26.14
l_{m2}	Average lengths of LV winding	cm	18.22
G_{cu1}	Weight of the HV winding	kg	2.69
G_{cu2}	Weight of the LV the winding	kg	0.45
P_{cu1}	Copper losses of the HV windings	Watt	6.72

P_{cu2}	Copper losses of the LV winding	Watt	3.96
G_{feb}	Weight of 3 legs of the transformer core	kg	2.06
G_{fej}	Weight of the transformer yoke	kg	5.3
P_{fej}	Iron loss of the transformer yoke	Watt	1.5
P_{feb}	Iron loss of 3 legs of the transformer core	Watt	2.153
G_{total}	Total weight of the transformer	kg	10.5
P_{total_loss}	Total loss of the transformer	Watt	14
η	Efficiency of the transformer	%	94.6

The design parameters are optimized in the PSO algorithm according to C and s values of the transformer. Therefore, efficiency and weight change of the transformer are performed as depending on the core quality factor and the current density of the windings.

4.2. Transformer optimization with Particle Swarm Optimization (PSO)

PSO method has been successfully used for solving different optimization problems including function optimization problems, efficiency and weight analysis etc. The method provides efficiency and weight optimization of the transformer depending on the C and s values. The transformer losses are minimized and the efficiency is maximized thanks to the optimization method. In addition, optimization of winding size creates a more efficient and cost-effective transformer model.

In the PSO algorithm, it is necessary to determine how many iterations it will usually work when applying to an optimization problem. The iteration is important to determine the least weight and most efficient state of the products. The PSO reaches the optimum solution in 30 iterations for this study. The transformer efficiency optimization result based on boundary conditions (s and C values) of the transformer is given in Figure 4.2.

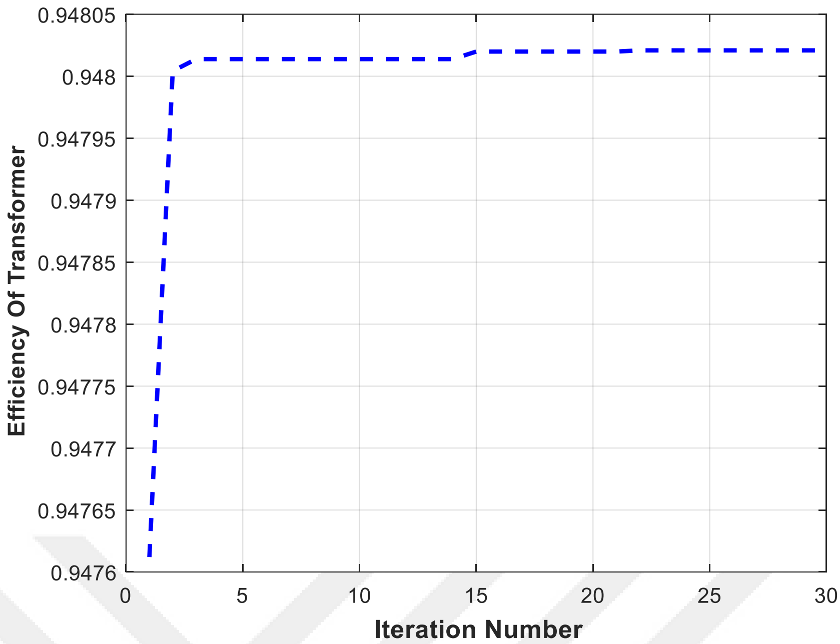

Figure 4.2. Maximum efficiency optimization of the analyzed 3-phase dry-type transformer with the PSO algorithm.

Figure 4.2 shows that the transformer reaches its maximum efficiency value at the values of the C=0.7 and s=2.2. These values obtained at the maximum efficiency of the transformer are given in detail at the following table.

Table 4.2. C and s values obtained at the maximum efficiency point of the transformer.

$\eta_{maximum}$	0.948018481095276
C	0.700169217033741
s	2.200399665246449

With resulting of the optimization shown in Figure 4.3, the minimum efficiency of the transformer (η=0.91) is obtained at the values of the C=1.499and s=3.499.

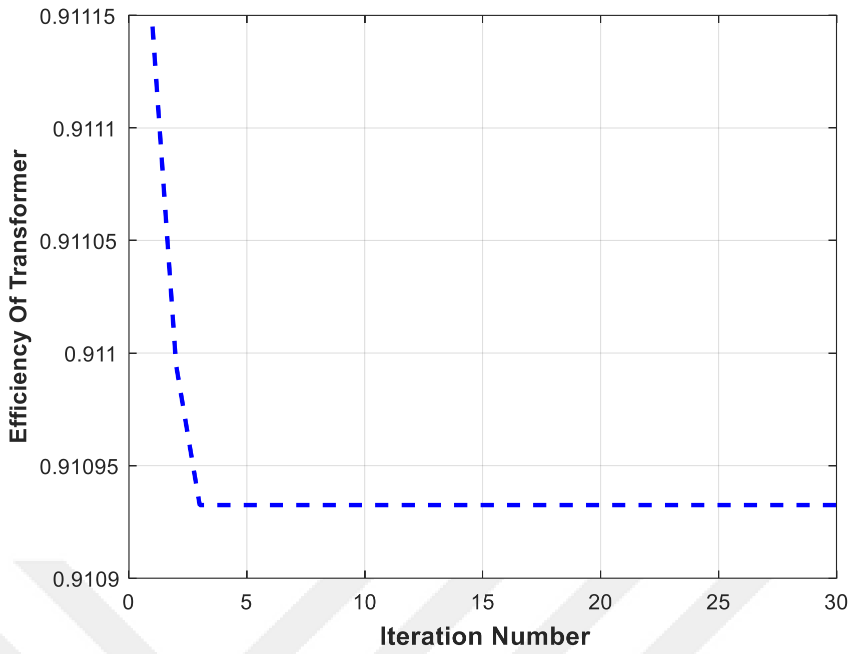

Figure 4.3. Minimum efficiency optimization of the analyzed 3-phase dry-type transformer with the PSO algorithm.

C and s values obtained at the minimum efficiency of the transformer are given in detail at the following table.

Table 4.3. C and s values obtained at the minimum efficiency point of the transformer.

$\eta_{minimum}$	0.910910543218883
C	1.499899467780051
s	3.499810409908549

Graphs and values of 3-dimensional analysis of efficiency are shown in Figure 4.4.

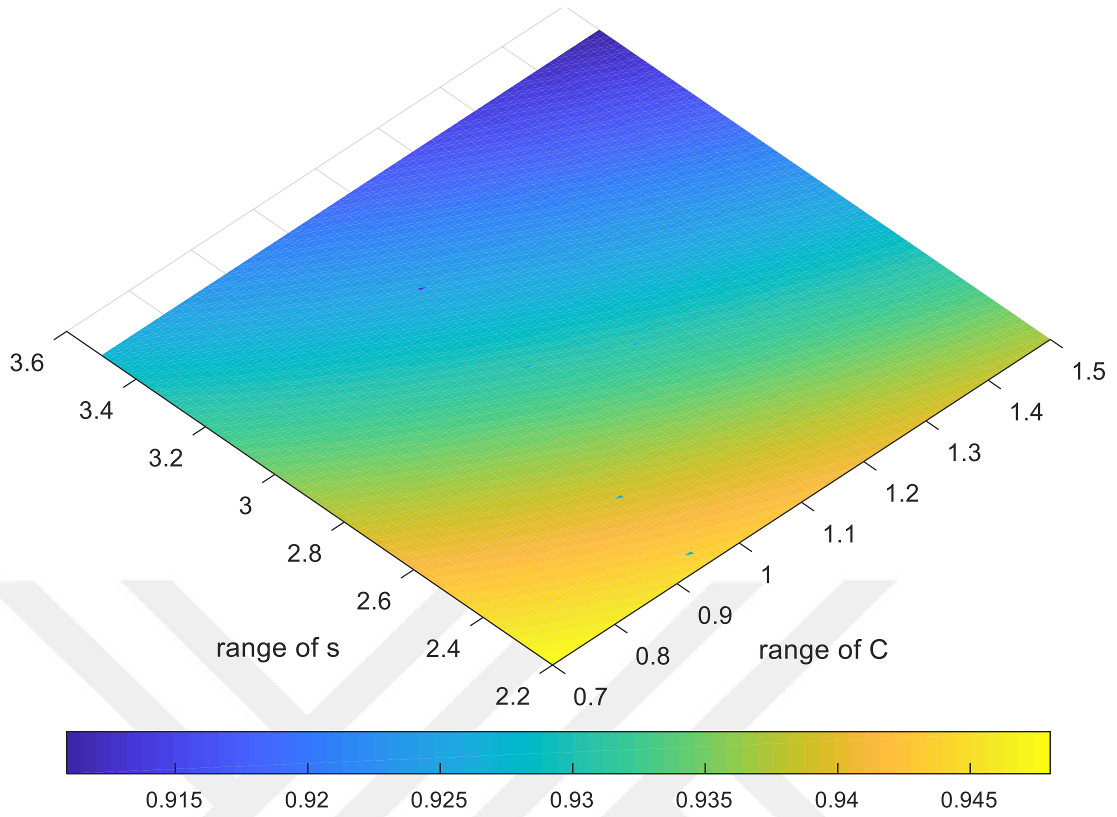

Figure 4.4. Change of transformer efficiency according to the current density (s) values corresponding to the core quality factor (C).

When considering Figure 4.4, it is shown that the maximum value of the efficiency is the parts where the light yellow is found. Where C_{min} = 0.7 and s_{min} = 2.2, the efficiency can be read from color-bar properties where η_{max} = 0.948 and η_{min} = 0.9109. Color-bar values of Figure 4.4 are given in Figure 4.5.

```
ColorBar with properties:

  Location: 'southoutside'
    Limits: [0.910905116737364 0.948027878564956]
  FontSize: 9
  Position: [0.130000000000000 0.151142857142857 0.775000000000000 0.050793650793651]
     Units: 'normalized'

Show all properties
```

Figure 4.5. Color-bar properties of transformer efficiency according to the current density (s) values corresponding to the core quality factor (C).

The values of the core quality factor and the current density are also related with the transformer's weight optimization parameters such as the specific weight of the copper and iron, a number of turns of the windings, cross-section area of the windings and the average lengths of upper and lower voltage windings. Hence, the weight optimization of the transformer is directly proportional to the cost of the transformer. The weight optimization of the transformer depending on the C and s values are given in the following figures.

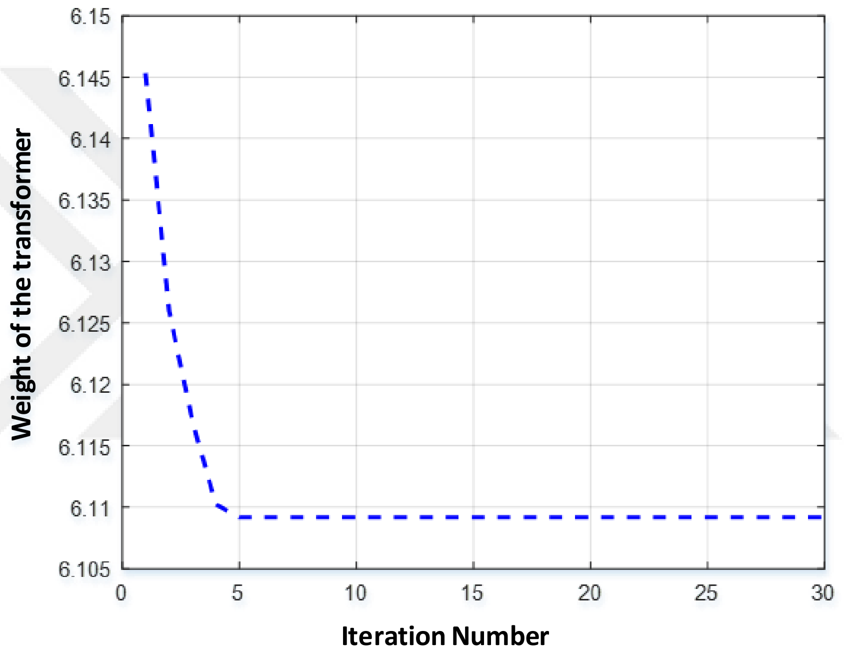

Figure 4.6. Determination of the transformer's minimum weight value with the PSO algorithm.

When considering the weigh optimization results, the minimum weight of the transformer (G=6.109) is obtained at the values of the C=0.7 and s=3.498.

Table 4.4. C and s values obtained at the minimum weight point of the transformer.

$G_{minimum}$	6.109170430858176
C	0.700077427294279
s	3.498784077540051

C and s values obtained at the minimum weight of the transformer are given in Table 4.4.

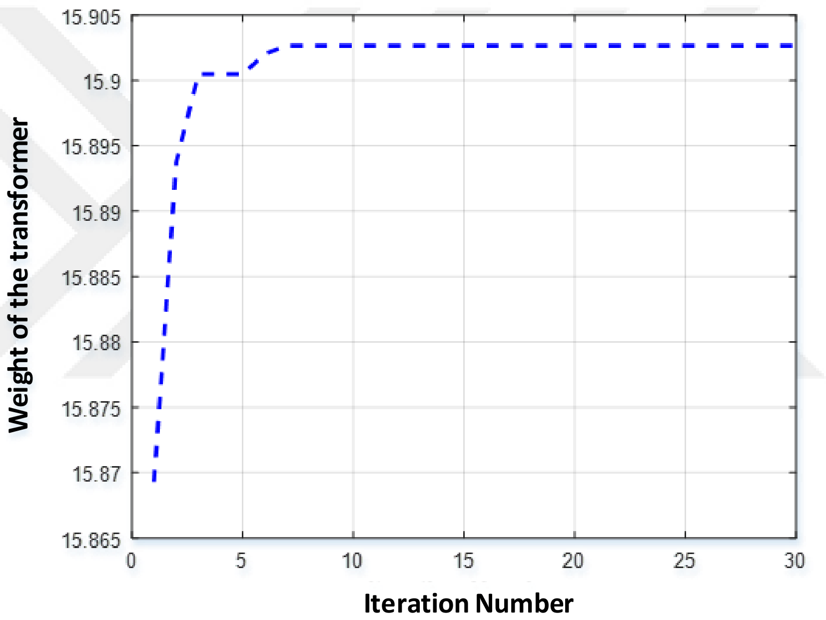

Figure 4.7. Determination of the transformer's maximum weight value with the PSO algorithm.

When Figure 4.7 is examined, it is seen that The maximum weight of the transformer (G=15.9) is obtained at the values of the C=1.5 and s=2.2.

Table 4.5. C and s values obtained at the maximum weight point of the transformer.

$\mathbf{G}_{maksimum}$	15.905572270726479
C	1.499927848899869
s	2.200090990303551

C and s values obtained at the minimum weight of the transformer are given in Table 4.5.

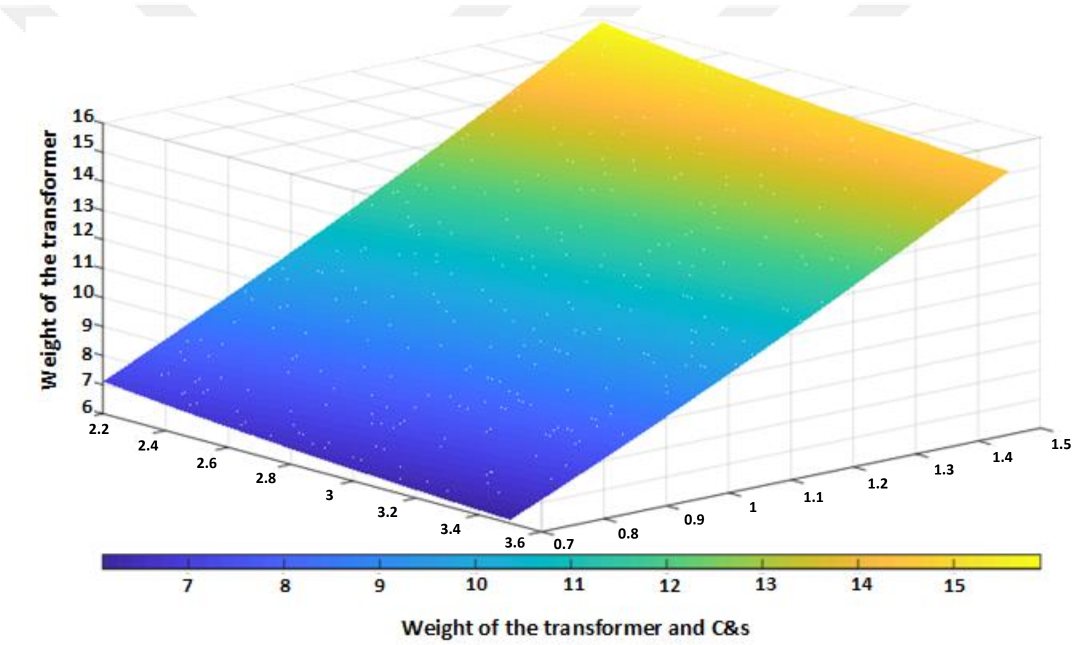

Figure 4.8. Change of the transformer's weight according to the current density (s) values corresponding to the core quality factor (C).

When Figure 4.8 is examined, the minimum value of the weight is obtained in the dominant parts of dark blue and navy blue tones. Where $C_{min} = 0.7$ and $s_{min} = 3.5$ are the minimum value for weight $G_{min} = 6.107868$. The maximum value that the weight can reach is read from color bar properties where $G_{max} = 15.90659$. Color-bar properties code generation is shown in Figure 4.9.

```
ColorBar with properties:

  Location: 'southoutside'
    Limits: [6.107868007087735 15.906597228106916]
  FontSize: 9
  Position: [0.130000000000000 0.151142857142857 0.775000000000000 0.050793650793651]
     Units: 'normalized'

Show all properties
```

Figure 4.9. Color-bar properties of transformer weight according to the current density (s) values corresponding to the core quality factor (C).

As a result of the optimization study, the maximum efficiency and the minimum weight are obtained at C = 0.7 during the optimization. However, the change in s value has opposite effects for yield and weight. When the current density is selected minimum, it gives maximum efficiency. When it is selected maximum, the minimum weight is available. The current density and the core quality factor to be chosen must be decided by considering the economic criteria of the transformer manufacturer or designer. For C = 0.7, the effects of the change of ‘s’ on efficiency and weight are shown in Table 4.6.

Table 4.6. Effects of the change of ‘s’ on efficiency and weight for C= 0.7.

Number	‘s’	Efficiency Change	Weight Change
1	**2.2000**	**0.9480**	**7.1039**
2	2.2500	0.9472	7.0443
3	2.3000	0.9464	6.9873
4	2.3500	0.9456	6.9327
5	2.4000	0.9448	6.8804
6	2.4500	0.9439	6.8303
7	2.5000	0.9431	6.7821
8	2.5500	0.9423	6.7358
9	2.6000	0.9415	6.6913
10	2.6500	0.9407	6.6485
11	2.7000	0.9399	6.6073
12	2.7500	0.9391	6.5676
13	2.8000	0.9383	6.5293
14	2.8500	0.9375	6.4923
15	2.9000	0.9367	6.4566

16	2.9500	0.9359	6.4221
17	3.0000	0.9351	6.3888
18	3.0500	0.9343	6.3566
19	3.1000	0.9335	6.3254
20	3.1500	0.9327	6.2952
21	3.2000	0.9319	6.2659
22	3.2500	0.9311	6.2375
23	3.3000	0.9303	6.2100
24	3.3500	0.9295	6.1833
25	**3.4000**	**0.9287**	**6.1574**

When the table is examined, 's' value which is close to the minimum weight can be selected by making concessions from the maximum efficiency value or vice versa. The design parameters obtained at the maximum efficiency of the transformer is given in Table 4.7.

Table 4.7. Design parameters of the transformer at the maximum efficiency point.

Symbols	Parameters	Units	Values
S_2	Secondary Apparent Power	VA	250
$U_{1\phi}$	Primary Phase Voltage	V	220
$U_{2\phi}$	Secondary Phase Voltage	V	63.5
q_{fe}	Core section of the transformer	cm^2	9.03
s	**Current density**	**A/cm^2**	**2.2**
C	**Transformer core section acceptability**	**-**	**0.7**
w_1	Primary Windings	turns	315
w_2	Secondary Windings	turns	91
I_1	Primary Current	A	0.4
I_2	Secondary Current	A	1.31
D	Diameter of a leg of transformer core	cm	4.15
q_1	Primary Winding Cross Section	mm^2	0.18
q_2	Secondary Winding Cross Section	mm^2	0.58
L_s	Window height of the core	cm	6.72

a	Window width of the transformer core	cm	2.74
l_{m1}	Average lengths of HV winding	cm	22.46
l_{m2}	Average lengths of LV winding	cm	14.53
P_{cu1}	Copper losses of the HV windings	Watt	6.59
P_{cu2}	Copper losses of the LV winding	Watt	3.46
P_{fej}	Iron loss of the transformer yoke	Watt	1.49
P_{feb}	Iron loss of 3 legs of the transformer core	Watt	2.15
P_{total_loss}	Total loss of the transformer	Watt	13.75
η	Efficiency of the transformer	%	94.85

The design parameters obtained at the minimum weight of the transformer is given in Table 4.8.

Table 4.8. Design parameters of the transformer at the minimum weight point.

Symbols	Parameters	Units	Values
S_2	Secondary Apparent Power	VA	250
$U_{1\phi}$	Primary Phase Voltage	V	220
$U_{2\phi}$	Secondary Phase Voltage	V	63.5
q_{fe}	Core section of the transformer	cm^2	9.03
s	**Current density**	**A/cm^2**	**3.499**
C	**Transformer core section acceptability**	**-**	**0.7**
w_1	Primary Windings	turns	312
w_2	Secondary Windings	turns	90
I_1	Primary Current	A	0.4
I_2	Secondary Current	A	1.31
D	Diameter of a leg of transformer core	cm	4.1
q_1	Primary Winding Cross Section	mm^2	0.11
q_2	Secondary Winding Cross Section	mm^2	0.37
L_s	Window height of the core	cm	6.7

a	Window width of the transformer core	cm	1.72
l_{m1}	Average lengths of HV winding	cm	23.48
l_{m2}	Average lengths of LV winding	cm	15.56
G_{cu1}	Weight of the HV winding	kg	0.25
G_{cu2}	Weight of the LV the winding	kg	1.44
G_{feb}	Weight of 3 legs of the transformer core	kg	1.38
G_{fej}	Weight of the transformer yoke	kg	3.03
G_{total}	Total weight of the transformer	kg	6.1

A 250 VA 380/110 V 3-phase dry-type transformer optimization parameters obtained by using PSO method. When considering all of these results, the transformer is efficiently designed and analyzed in ANSYS/Maxwell program.

4.3. Electromagnetic and thermal analysis of the transformer in ANSYS/Maxwell

Dry-type transformers are the significant parts of the electrical machines that do not require a liquid such as oil or silicone or any other liquid to cool its core and windings. Therefore, these transformers are overheated at the load and overload conditions in a short time. Overheating of the transformer results in the rapid deterioration of the insulation materials, insulation aging, iron and copper losses related to efficiency reduction and the complete failure of the transformer. In order to observe the electromagnetic and thermal changes on the transformer, 250 VA 380/110 V 3-phase dry-type transformer is designed and analyzed in ANSYS/Maxwell program. The design process is provided by using optimization parameters of the transformer.

For modeling of the transformer, the design steps in ANSYS/Maxwell program are as follows:

- Maxwell-3D operation is selected to create a 3D model of the transformer.

- An optimal solution type of model is defined. These solvers consist of magnetic and electrostatic solutions.

- The transformer is modeled as its dimensions by using 3D objects.
- The transformer core and windings materials type are selected in the properties panel.
- Boundary and excitation data of the transformer core and coil terminals are formed in detail.
- Mesh operation is created on all materials of the transformer.
- Boundaries and duration time of the analysis are determined in the analysis setup panel.
- After the analysis is started, analysis results, report data and the diagrams are obtained in the results panel.

Firstly, the transformer is modeled as 3D so the transformer core, primary and secondary windings of the transformer are designed by using Maxwell-3D shown in Figure 4.10.

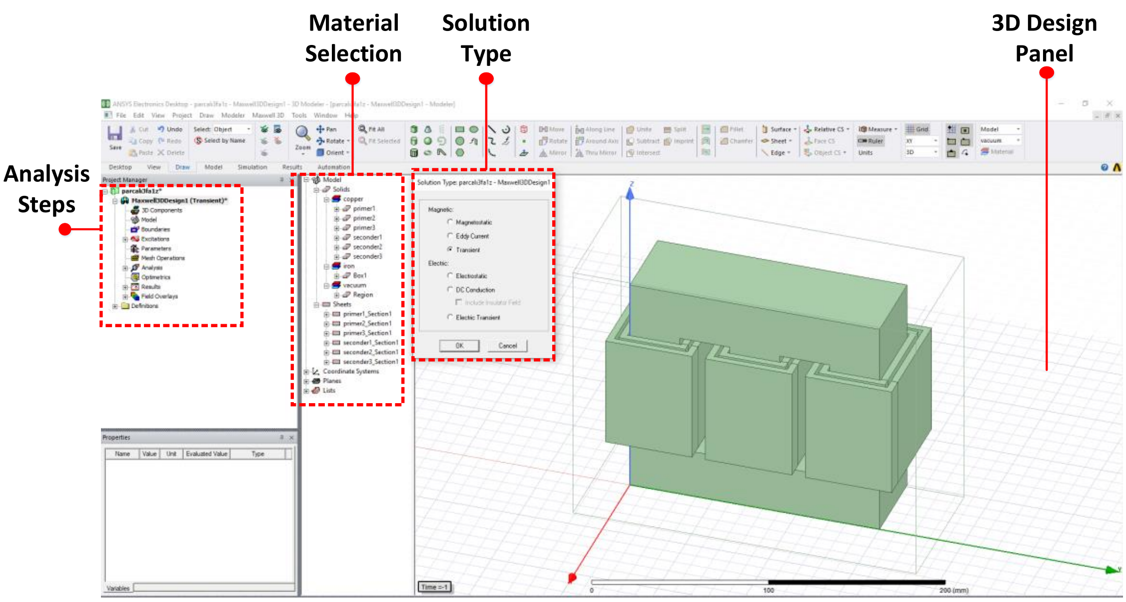

Figure 4.10. ANSYS/Maxwell 3D design operation panel.

The solution type of creating design is selected as magnetic-transient. Because the transformers are the electromagnetic devices and analysis results are performed depending on the time. Then, the transformer core and windings are modeled by using 3D-solid objects. Designed transformer model is given in Figure 4.11.

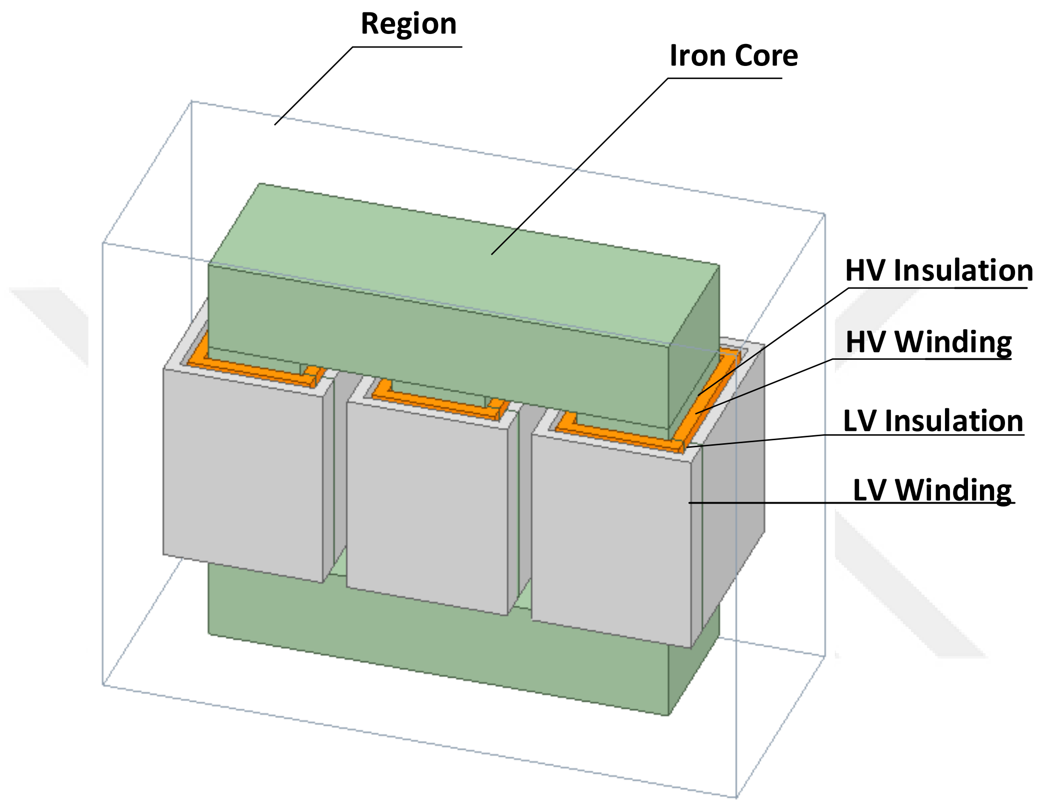

Figure 4.11. ANSYS Maxwell design of 250 VA 380/110 V 3-phase dry-type transformer.

After modeling of the transformer core and windings, material types of this equipment is selected by using the material property panel shown in Figure 4.12a.

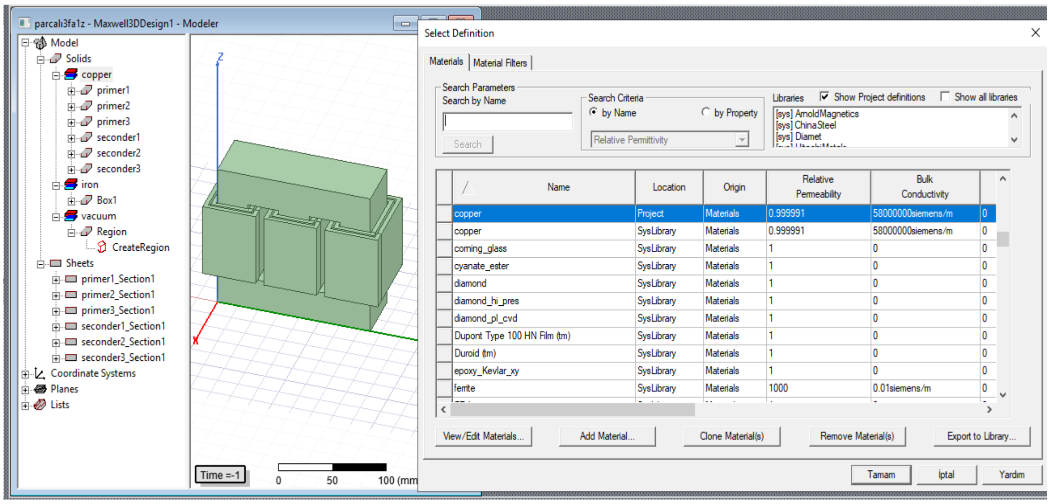
parcali3fa1z - Maxwell3DDesign1 - Modeler
Model
Solids
copper
primer1
primer2
primer3
seconder1
seconder2
seconder3
iron
Box1
vacuum
Region
CreateRegion
Sheets
primer1_Section1
primer2_Section1
primer3_Section1
seconder1_Section1
seconder2_Section1
seconder3_Section1
Coordinate Systems
Planes
Lists
Select Definition
Materials
Material Filters
Search Parameters
Search by Name
Search Criteria
by Name
by Property
Relative Permittivity
Libraries
Show Project definitions
Show all libraries
[sys] AmoldMagnetics
[sys] ChinaSteel
[sys] Diamet
Search
Name
Location
Origin
Relative Permeability
Bulk Conductivity
copper
Project
Materials
0.999991
58000000siemens/m
copper
SysLibrary
Materials
0.999991
58000000siemens/m
coming_glass
cyanate_ester
diamond
diamond_hi_pres
diamond_pl_cvd
Dupont Type 100 HN Film (tm)
Duroid (tm)
epoxy_Kevlar_xy
ferrite
1000
0.01siemens/m
View/Edit Materials...
Add Material...
Clone Material(s)
Remove Material(s)
Export to Library...
Tamam
İptal
Yardım
Time =-1
0
50
100 (mm

(a)

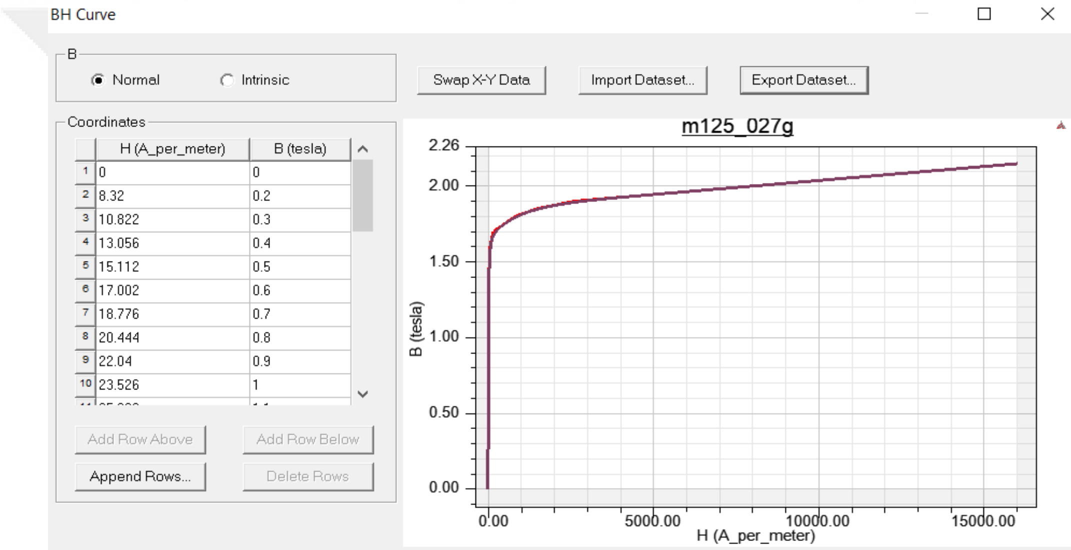
BH Curve
B
Normal
Intrinsic
Swap X-Y Data
Import Dataset...
Export Dataset...
Coordinates
H (A_per_meter)
B (tesla)
1 0 0
2 8.32 0.2
3 10.822 0.3
4 13.056 0.4
5 15.112 0.5
6 17.002 0.6
7 18.776 0.7
8 20.444 0.8
9 22.04 0.9
10 23.526 1
Add Row Above
Add Row Below
Append Rows...
Delete Rows
m125_027g
2.26
2.00
1.50
1.00
0.50
0.00
B (tesla)
0.00
5000.00
10000.00
15000.00
H (A_per_meter)

(b)

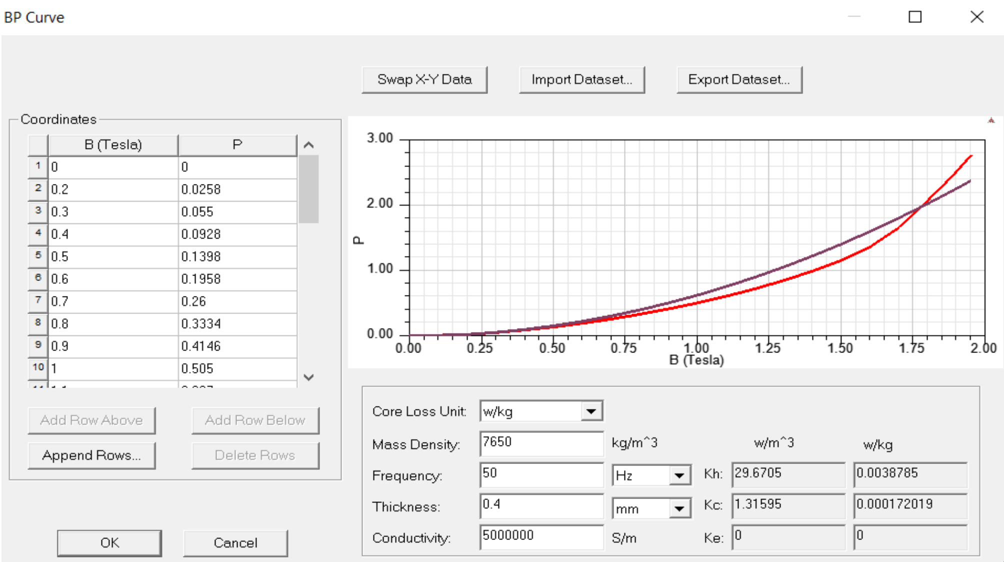
BP Curve
Swap X-Y Data
Import Dataset...
Export Dataset...
Coordinates
B (Tesla)
P
1 0 0
2 0.2 0.0258
3 0.3 0.055
4 0.4 0.0928
5 0.5 0.1398
6 0.6 0.1958
7 0.7 0.26
8 0.8 0.3334
9 0.9 0.4146
10 1 0.505
Add Row Above
Add Row Below
Append Rows...
Delete Rows
3.00
2.00
1.00
0.00
P
0.00
0.25
0.50
0.75
1.00
1.25
1.50
1.75
2.00
B (Tesla)
Core Loss Unit:
w/kg
Mass Density:
7650
kg/m^3
w/m^3
w/kg
Frequency:
50
Hz
Kh:
29.6705
0.0038785
Thickness:
0.4
mm
Kc:
1.31595
0.000172019
Conductivity:
5000000
S/m
Ke:
0
0
OK
Cancel

(c)

Figure 4.12. Material property panel (a) determining of material type of the region, transformer core and windings (b) B-H curve of the iron core (c) B-P loss curve characteristic features of the iron core.

During the design process, the core material of the transformer is selected as iron. The iron characteristic features are determined in detail. These characteristics are the relative permeability related to a magnetic field – magnetic field vector (B-H) curve and magnetic field – loss (B-P) curve of the transformer core shown in Figure 4.12b and 4.12c. Moreover, the primary and secondary windings of the transformer are selected as copper material. Mass density, bulk conductivity and Poisson's ratio properties of the copper are defined specially. Finally, the air material is assigned as a region or a boundary because of the dry characteristic of the transformer.

After the assigning of the materials, primary and secondary windings of the transformers are excited and energized according to the transformer parameters. These windings are designed by considering their turn ratio, ohmic resistance and excitation terminal voltage values. Excitation assignment of the windings is shown in Figure 4.13.

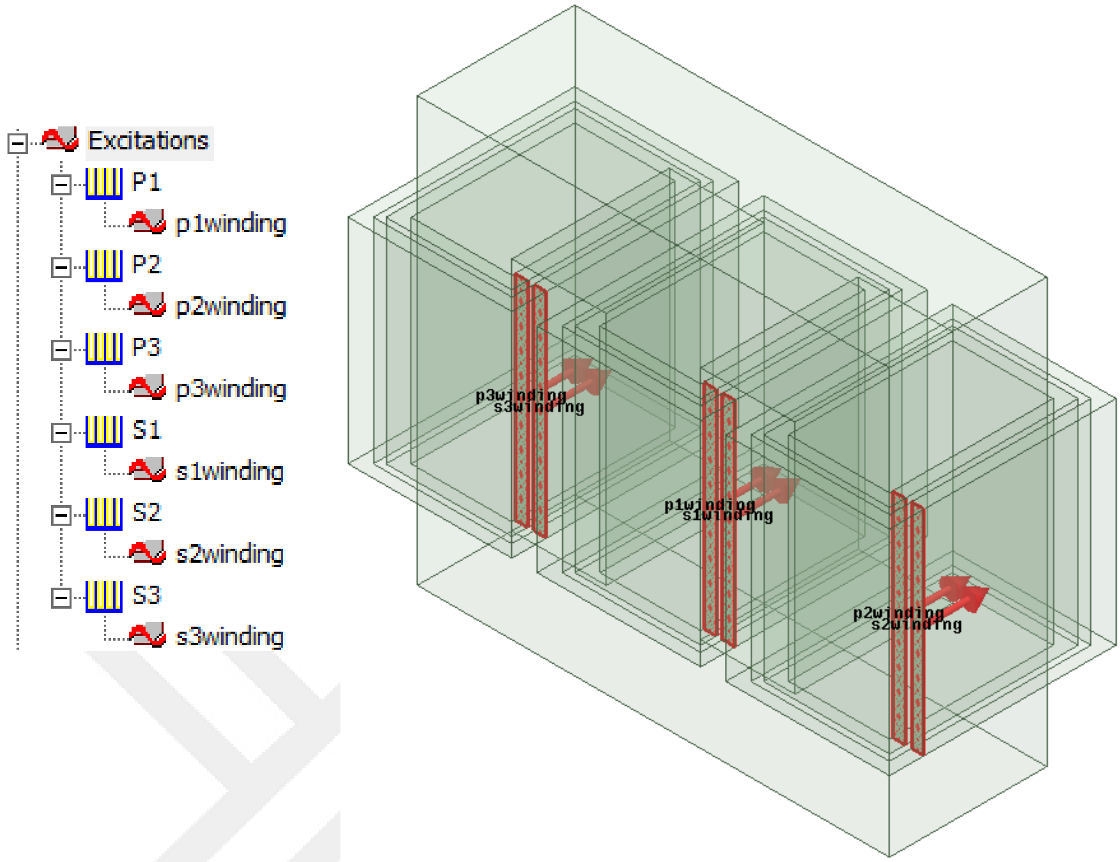

Figure 4.13. Assignment of excitation to the coil terminals of the transformer.

After the material properties of the transformer are selected, mesh operation is applied to the transformer core and coils. This operation is the most important part of the analysis process because it allows a physical definition range to be divided into smaller definition ranges (elements). The designed transformer is divided into a hundred thousand (100000) particles thanks to mesh operation so all particles are electromagnetically analyzed. The designed model is analyzed more accurately thanks to the mesh operation. The mesh operation on the transformer model is given in Figure 4.14.

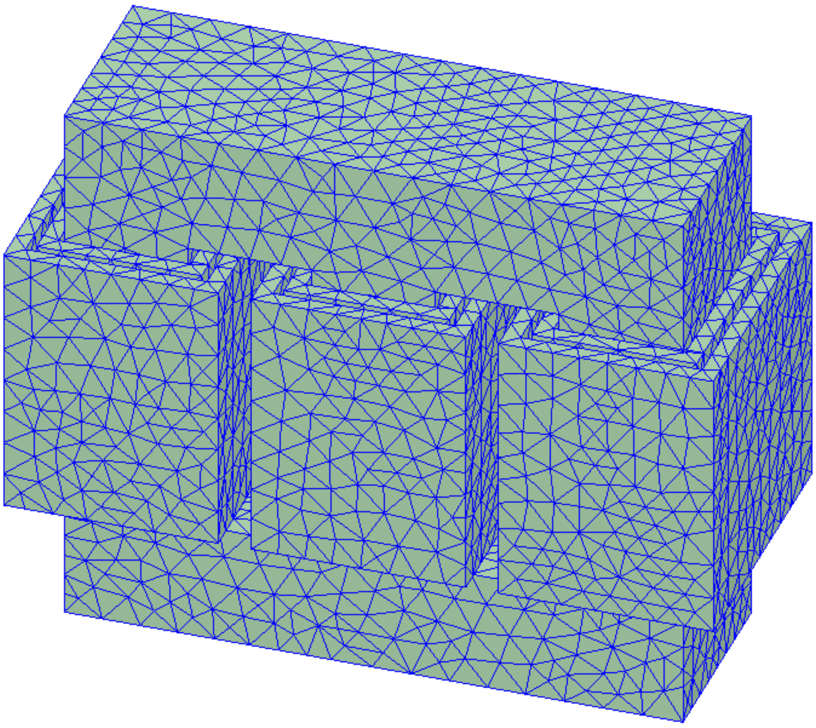

Figure 4.14. Mesh operation applied to the core and windings of the transformer.

At the end of all of these process, the transformer is ready for analyzing. Analysis time should be determined by using the setup panel. Analysis solution step, type, start and stop time parameters are defined accurately. These parameters are the key parameters to solve the electromagnetic transient analysis of the transformer because they directly affect the accuracy of the currents, voltages and losses signals on the transformer. Analysis step size for this study is selected small ranges in order to obtain pure signals. The analysis setting of the transformer is given in Figure 4.15.

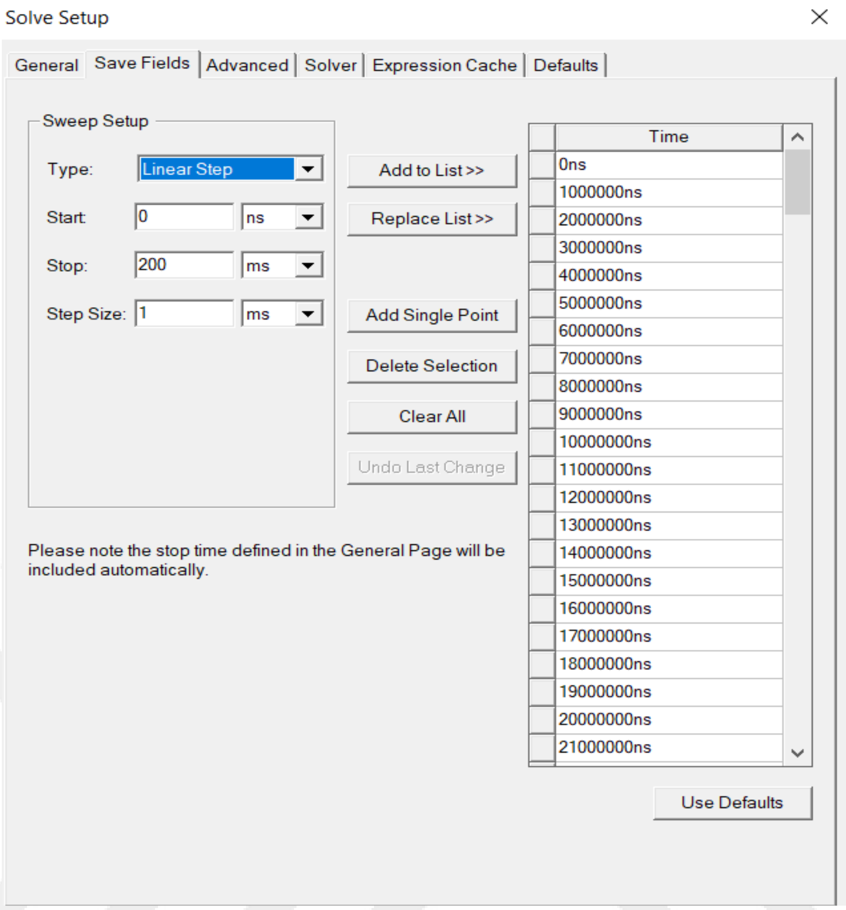

Figure 4.15. Analysis settings of the transformer in ANSYS/Maxwell.

Finally, analysis results are obtained depending on the analysis time. The electromagnetic transient analysis results are presented as follows.

When a voltage is applied to the primary side of coils, a changing magnetic field occurs on the transformer core and coils. This magnetic field induces a voltage across the ends of the coil. Changing a magnetic field in the primary coil changes the current and also the magnetic flux. The changing magnetic flux induces a voltage in the secondary side of the coils. The magnetic flux distribution on the analyzed transformer core is given in Figure 4.16.

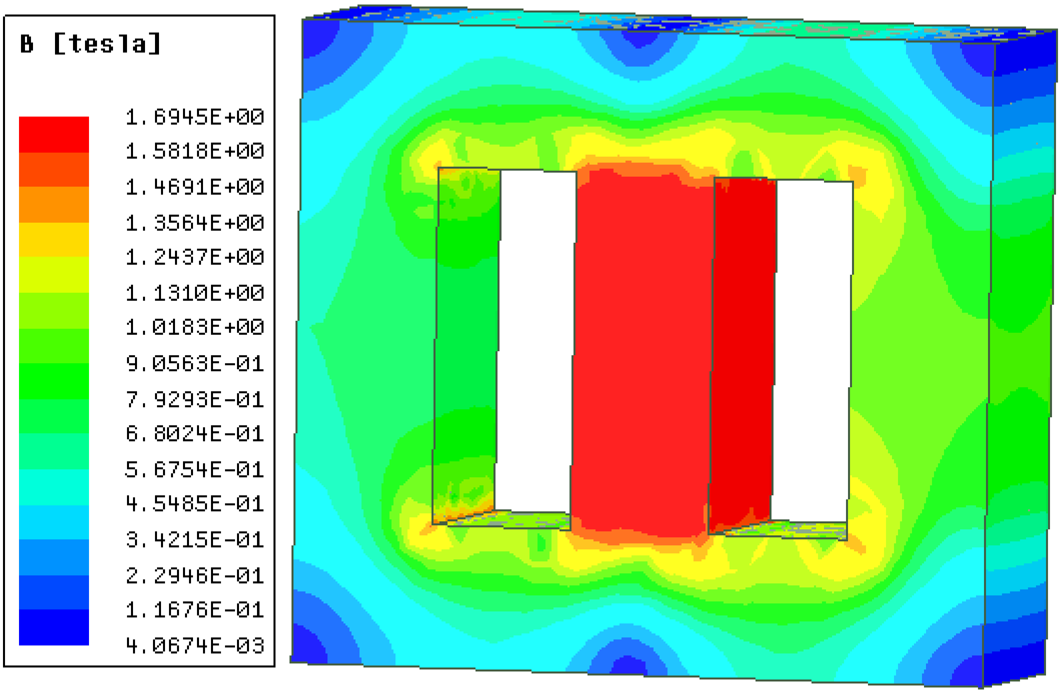

Figure 4.16. Magnetic field distribution on the transformer core.

The transformer is tested at the load and overload condition. When 380 volts is applied to the primary side of the coils, 110 volts are induced in the secondary side of the coils at load condition. The primary and secondary voltages and currents of the designed transformer are shown in Figure 4.17 and Figure 4.18.

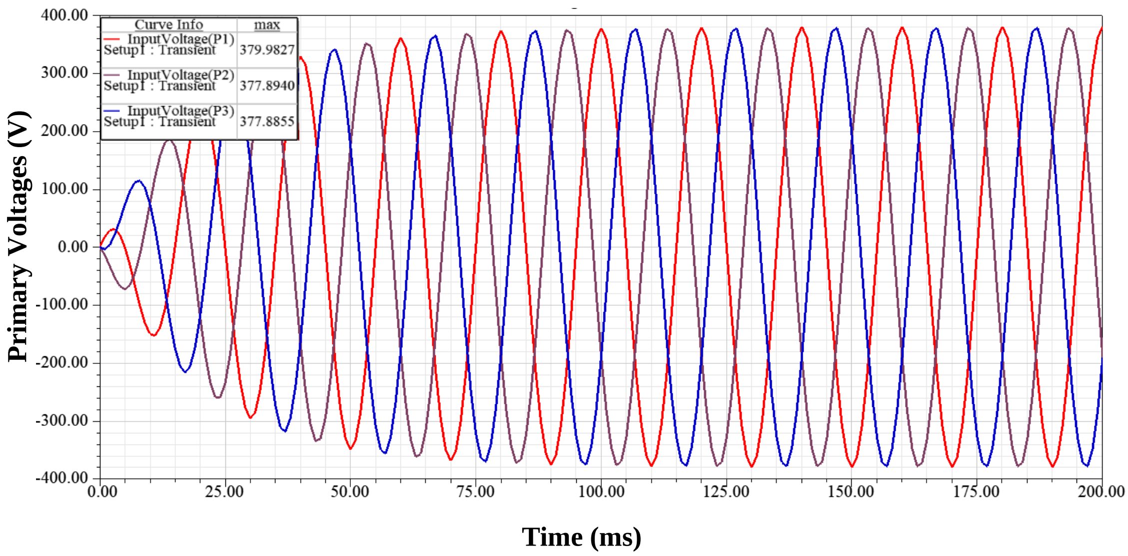

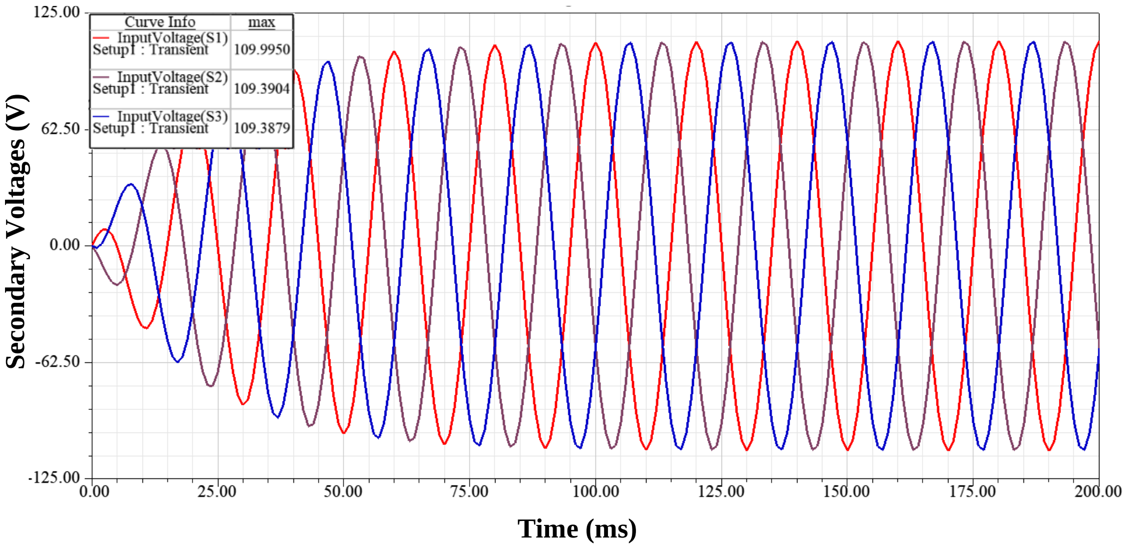

Figure 4.17. Primary and secondary voltages of the 250 VA 380/110-V 3-phase dry-type transformer.

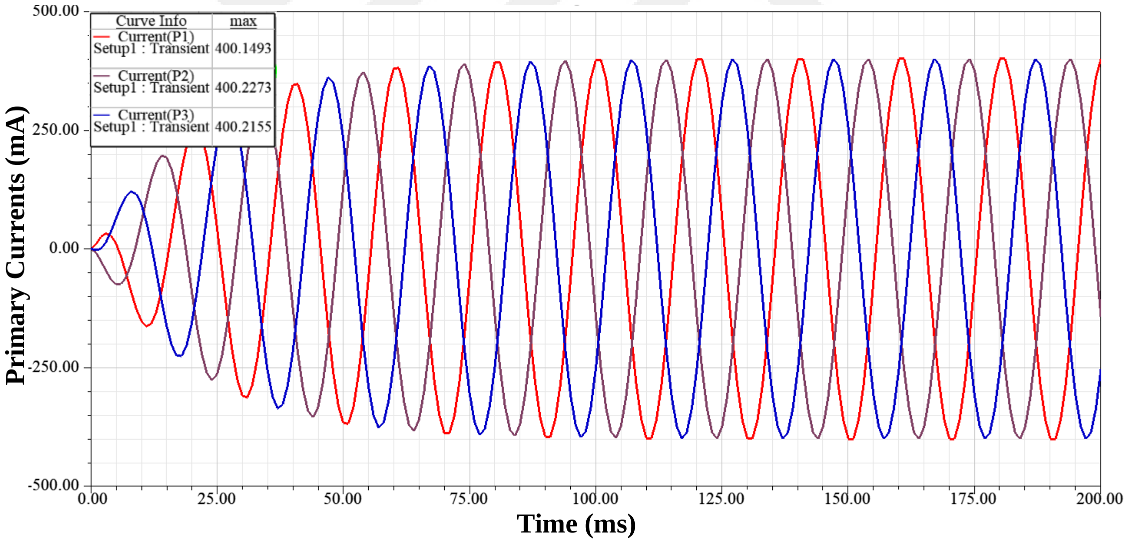

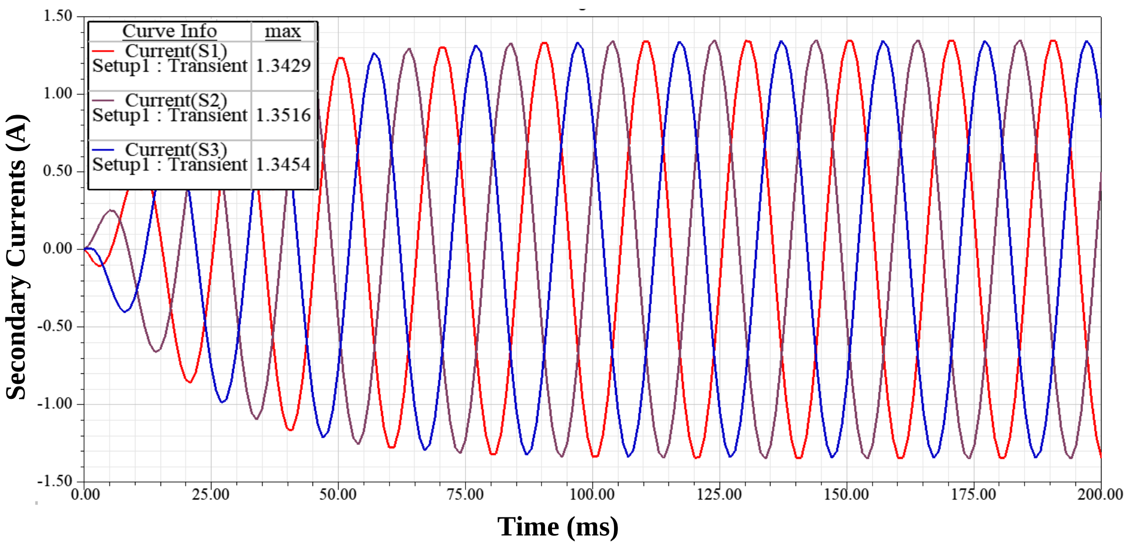

Figure 4.18. Primary and secondary currents of the 250 VA 380/110-V 3-phase dry-type transformer.

Another analysis result is the transformer losses that are eddy current, hysteresis and core losses. These losses are occurred by the heating of the transformer, nonlinearity of the transformer core and the resistance of the windings. Figure 4.19 shows the losses characteristic of the analyzed transformer.

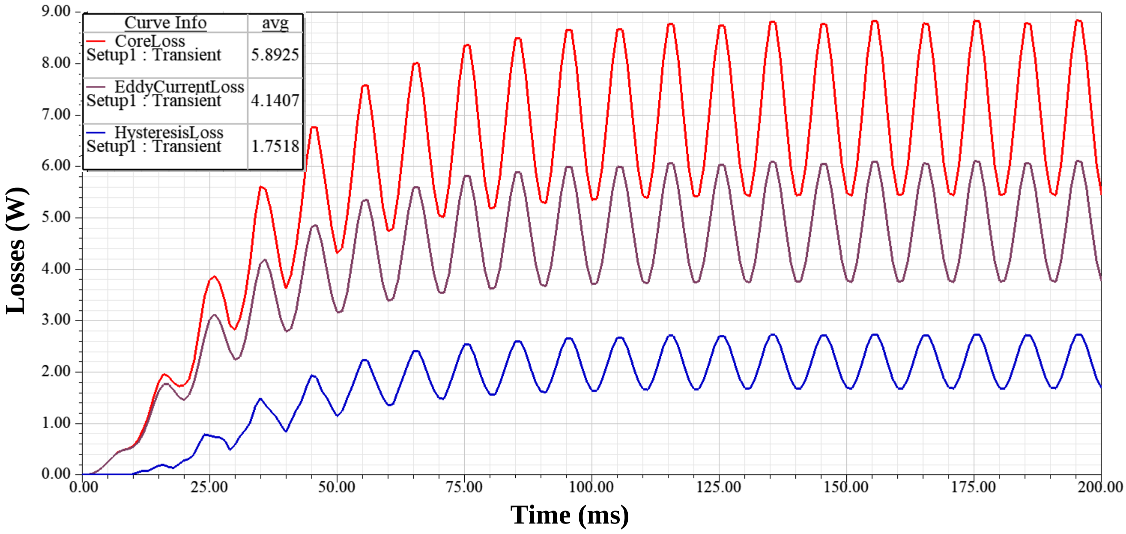

Figure 4.19. Core, eddy current and hysteresis losses of the 250 VA 380/110-V 3-phase dry-type transformer.

The transformer is analyzed electromagnetically by ANSYS/Maxwell program. After the electromagnetic transient analysis of the transformer, it is also analyzed thermally in order to observe the temperature distribution on the core and windings. Temperature distribution analysis is a significant step for the dry-type transformers. Because temperature rises on the core and windings causes the deterioration of the insulation system and thermal aging of the transformer. Hence, the transformer is thermally analyzed in Maxwell program at the overloaded condition. Thermal analysis of the transformer is given in Figure 4.20.

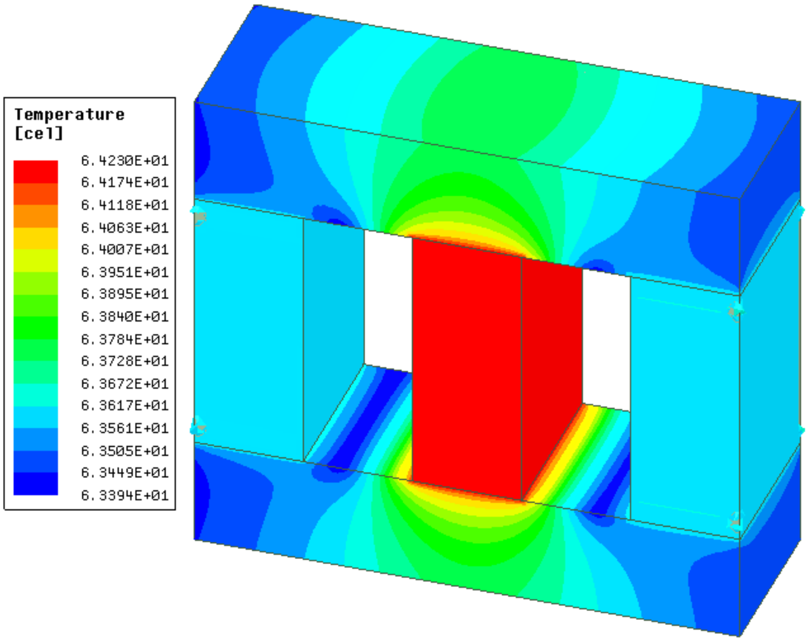

(a)

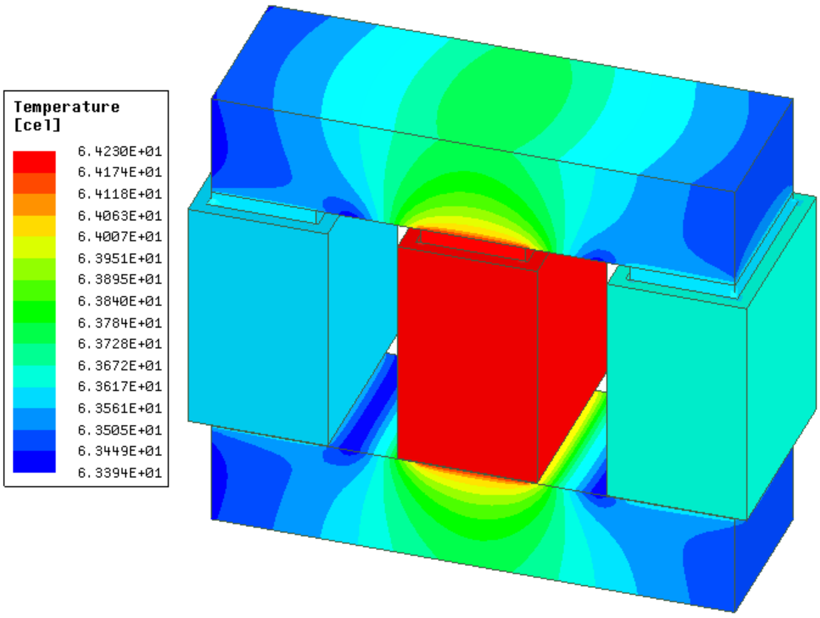

(b)

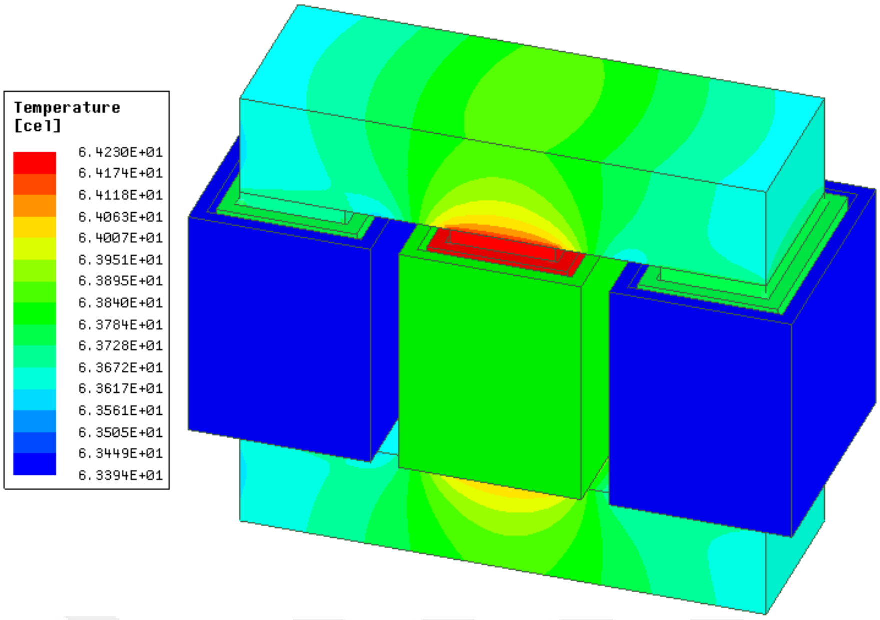

(c)

Figure 4.20. The temperature distribution of the transformer's (a) transformer core (b) primary windings of the transformer (c) secondary windings of the transformer.

The transformer is designed and analyzed by the ANSYS/Maxwell program. It is also optimized via PSO algorithm by using mathematical model parameters of the dry-type transformer. In order to verify the simulation results, it is a necessary operation for testing of the analyzed transformer. Hence, the designed transformer is manufactured to test at the load and overload condition in the laboratory.

4.4. Experimental analysis of the transformer

The designed transformer is tested by setting up an experiment unit in the laboratory. Thermal measurements of the transformer are measured at 6 different points of the transformer. The measurements and temperature distribution on the transformer are observed by using a thermal imaging camera (Testo-881). Thermal measurements are recorded as centigrade degree (°C) by the PLC measurement stations and also monitored simultaneously in the HMI (Human Machine Interface) panel. Gathered data from the measurement station is shown in Table 4.9.

Table 4.9. Thermal measurement data of the transformer at load and overload condition.

Id	Time	Primary Windings (Left and Right Leg)	Secondary Windings (Left and Right Leg)	Middle leg of The Primary Winding	Middle Leg of The Core	Left Leg of The Core	Right Leg of The Core
1	29.11.2018 11:46	36,2	37,1	39,3	35,1	26,8	28,4
2	29.11.2018 11:47	36,2	36,4	39,3	35,3	26,9	28,3
3	29.11.2018 11:48	36,7	37,2	39,2	35,2	27	28,3
4	29.11.2018 11:49	36,7	37,1	39,6	35,6	27,1	28,9
5	29.11.2018 11:50	36,8	36,8	40,2	35,7	27,1	28,7
6	29.11.2018 11:51	37,1	37,2	40	35,7	27,3	28,6
7	29.11.2018 11:52	37,2	37	40,5	35,6	27,5	28,6
8	29.11.2018 11:53	37,5	37,4	40,5	35,7	27,4	28,8
9	29.11.2018 11:54	37,6	37,1	40,9	36,1	27,7	28,8
10	29.11.2018 11:55	37,8	37,5	41,1	35,8	27,9	29
11	29.11.2018 11:56	37,9	37,2	41,3	36,3	27,7	28,9
12	29.11.2018 11:57	38,1	37,8	41,6	36,4	27,9	29,1
13	29.11.2018 11:58	38,1	37,8	42,1	36,3	28,1	29,2
14	29.11.2018 11:59	38,2	37,7	42,2	36,4	28,2	29,1
15	29.11.2018 12:00	38,4	37,3	42,2	36,4	28,4	29,1
16	29.11.2018 12:01	38,6	37,7	42,6	36,7	28,4	29,5
17	29.11.2018 12:02	38,7	37,5	42,9	37	28,6	29,1
18	29.11.2018 12:03	38,9	37,8	42,8	37	28,5	29,4
19	29.11.2018 12:04	39	37,5	43	37	28,8	29,5
20	29.11.2018 12:05	39,1	38,1	43,5	37,2	28,7	29,5
21	29.11.2018 12:06	39,4	38,1	43,3	37,1	29	29,3

22	29.11.2018 12:07	39,4	38,6	43,4	37,1	29,1	29,5
23	29.11.2018 12:08	39,7	38,8	43,8	37,1	29,2	29,8
24	29.11.2018 12:09	39,8	38,8	43,9	37,4	29,1	29,6
25	29.11.2018 12:10	40,1	38,6	44	37,5	29,4	29,6
26	29.11.2018 12:11	40,2	39,4	44,4	37,3	29,3	29,9
27	29.11.2018 12:12	40,2	39,8	44,6	37,3	29,6	29,7
28	29.11.2018 12:13	40,5	39,6	44,4	37,4	29,6	29,8
29	29.11.2018 12:14	40,5	39,8	44,8	37,1	29,6	29,8
30	29.11.2018 12:15	40,9	39,5	44,8	37,2	29,8	30
31	29.11.2018 12:16	40,9	39,7	45,1	37,2	29,9	30,2
32	29.11.2018 12:17	41,1	39,4	45,1	37,6	29,9	30,2
33	29.11.2018 12:18	41,2	40,1	45,3	37,4	30,1	30,2
34	29.11.2018 12:20	41,3	40,5	45,6	37,6	30,1	30,7
35	29.11.2018 12:21	41,5	40	45,8	37,9	30,3	30,7
36	29.11.2018 12:22	41,5	40,4	46,3	37,8	30,4	30,6
37	29.11.2018 12:23	41,7	39,8	46,1	38	30,5	30,7
38	29.11.2018 12:24	41,6	40,3	46,5	37,9	30,5	31,1
39	29.11.2018 12:25	41,8	40,9	46,8	37,9	30,5	31
40	29.11.2018 12:26	42,1	40,7	46,9	38,1	30,7	30,5
41	29.11.2018 12:27	42	41	47	38,5	30,7	30,7
42	29.11.2018 12:28	42,4	41,3	46,5	38,6	30,7	30,7
43	29.11.2018 12:29	42,3	40,5	46,5	38,5	31	30,8
44	29.11.2018 12:30	42,4	40,3	47	38,8	31	30,9
45	29.11.2018 12:31	42,4	40,2	47,4	38,6	31,1	31,2
46	29.11.2018 12:32	42,5	40,8	47,3	38,5	31,1	31,2

47	29.11.2018 12:33	42,5	41	47,8	38,3	31,2	31,6
48	29.11.2018 12:34	42,8	41,1	47,9	38,2	31,3	31,5
49	29.11.2018 12:35	42,9	41,4	47,9	38,4	31,4	31,6
50	29.11.2018 12:36	43	41,6	47,9	38,6	31,4	31,4
51	29.11.2018 12:37	43,3	41,6	47,8	38,5	31,5	31,4
52	29.11.2018 12:38	43,1	41,5	48,1	38,6	31,5	31,6
53	29.11.2018 12:39	43	40,5	47,8	39,4	31,5	31,9
54	29.11.2018 12:40	43	40,8	48,2	39,7	31,5	32,4
55	29.11.2018 12:41	43,1	40,8	48,5	39,6	31,6	32,5
56	29.11.2018 12:42	43	40,4	48,5	39,6	31,9	32,6
57	29.11.2018 12:43	43,2	40,4	48,4	39,9	31,9	32,8
58	29.11.2018 12:44	43,3	40,4	48,8	39,7	31,9	32,8
59	29.11.2018 12:45	43,5	40,2	48,7	39,6	32	32,6
60	29.11.2018 12:46	43,5	40,9	48,7	39,2	32,1	33
61	29.11.2018 12:47	43,6	40,6	48,7	39,6	32,1	32,9
62	29.11.2018 12:48	43,7	41,4	49	39,4	32,4	33,1
63	29.11.2018 12:49	43,9	41,7	49,3	39,4	32,2	32,9
64	29.11.2018 12:50	44,2	42,2	49,2	39,5	32,3	32,7
65	29.11.2018 12:51	44,3	42,7	49,8	40,6	32,3	32,6
66	29.11.2018 12:52	44,4	43	49,5	41,4	32,4	33,1
67	29.11.2018 12:53	44,6	43	49,6	41,9	32,3	33,1
68	29.11.2018 12:54	44,6	43,5	49,8	41,6	32,4	33,1
69	29.11.2018 12:55	44,8	42,6	50,3	41,9	32,6	33,4
70	29.11.2018 12:56	44,6	42,3	50,1	42	32,5	33,7
71	29.11.2018 12:57	44,5	41,9	50	41,9	32,7	34,1

72	29.11.2018 12:58	44,5	41,8	50,5	42	32,7	34,1
73	29.11.2018 12:59	44,5	42,5	50,4	41,7	32,9	34,1
74	29.11.2018 13:00	44,7	42,4	50,2	41,8	33	34,6
75	29.11.2018 13:01	44,5	41,9	50,8	42	33	34,7
76	29.11.2018 13:02	44,7	41,9	50,5	42	33,2	34,7
77	29.11.2018 13:03	44,8	41,3	50,5	42	33,1	34,8
78	29.11.2018 13:04	44,8	40,9	50,8	41,7	33,4	34,7
79	29.11.2018 13:05	44,7	41,2	50,6	41,8	33,3	35
80	29.11.2018 13:06	44,8	41,2	50,7	41,9	33,2	34,9
81	29.11.2018 13:07	44,3	40,6	50,9	41,6	33,1	34,8
82	29.11.2018 13:08	43,5	39,5	50,8	40,9	33,1	34,6
83	29.11.2018 13:09	43,7	39,8	50,6	40,9	32,8	34,7
84	29.11.2018 13:10	43,2	39,1	50,7	40,5	32,4	34,7
85	29.11.2018 13:11	43	39	50,5	40	32,4	34,8
86	29.11.2018 13:12	42,8	39,2	50,5	39,8	32,2	34,8
87	29.11.2018 13:13	42,6	38,8	50,2	39,7	32,1	34,8
88	29.11.2018 13:14	42,4	38,5	50,1	39,5	31,9	34,9
89	29.11.2018 13:15	42,1	37,9	50	39	31,6	34,8
90	29.11.2018 13:16	42,4	38	50,2	39,1	31,2	34,9
91	29.11.2018 13:17	42,5	38,1	50	38,6	31,4	34,7
92	29.11.2018 13:18	43,3	39,7	50,4	39,4	31,2	34,6
93	29.11.2018 13:19	43,9	40,6	50,4	39,6	31,6	34,5
94	29.11.2018 13:20	44,2	40,6	50,6	40,1	31,9	34,5
95	29.11.2018 13:21	44,3	41,3	51	39,9	31,9	34,7
96	29.11.2018 13:22	44,3	41,4	51,2	40,1	32,1	34,8

97	29.11.2018 13:23	44,8	41,8	51,1	40,3	32,3	34,5
98	29.11.2018 13:24	44,9	41,8	51,8	40,6	32,5	34,6
99	29.11.2018 13:25	45	41,5	51,7	40,7	32,7	34,5
100	29.11.2018 13:26	45,1	42	51,8	40,8	32,7	34,6
101	29.11.2018 13:27	45,2	41,8	51,7	40,9	32,9	34,8
102	29.11.2018 13:28	45,2	42,3	51,9	40,9	33,1	34,9
103	29.11.2018 13:29	45,2	41,8	52,2	41	33,3	34,8
104	29.11.2018 13:30	45,2	42,1	52	41,5	33,3	35
105	29.11.2018 13:31	45,3	42	52,2	41,6	33,4	35,1
106	29.11.2018 13:32	45,3	42,4	52	41,4	33,5	34,9
107	29.11.2018 13:33	45,3	44,5	52,5	42,4	34,8	35,1
108	29.11.2018 13:48	45,7	47,3	53,8	43,6	36	35,5
109	29.11.2018 13:49	48,7	48,9	55,4	45,3	38	37,8
110	29.11.2018 13:50	50,5	50,7	57,2	47,1	39,8	39,6
111	29.11.2018 13:51	52,3	52,5	59	48,9	41,6	41,4
112	29.11.2018 13:52	54,1	54,3	60,8	50,7	43,4	43,2
113	29.11.2018 13:53	55,9	56,1	62,6	52,5	45,2	45
114	29.11.2018 13:54	57,7	57,9	64,4	54,3	47	46,8
115	29.11.2018 13:55	58	58,2	64,7	54,6	47,3	47,1
116	29.11.2018 13:55	58,3	58,5	65	54,9	47,6	47,4
117	29.11.2018 13:55	58,6	58,8	65,3	55,2	47,9	47,7
118	29.11.2018 13:55	58,9	59,1	65,6	55,5	48,2	48

Temperature distribution of the transformer is also obtained by the thermal imaging camera. The thermal image of the transformer is shown in Figure 4.21.

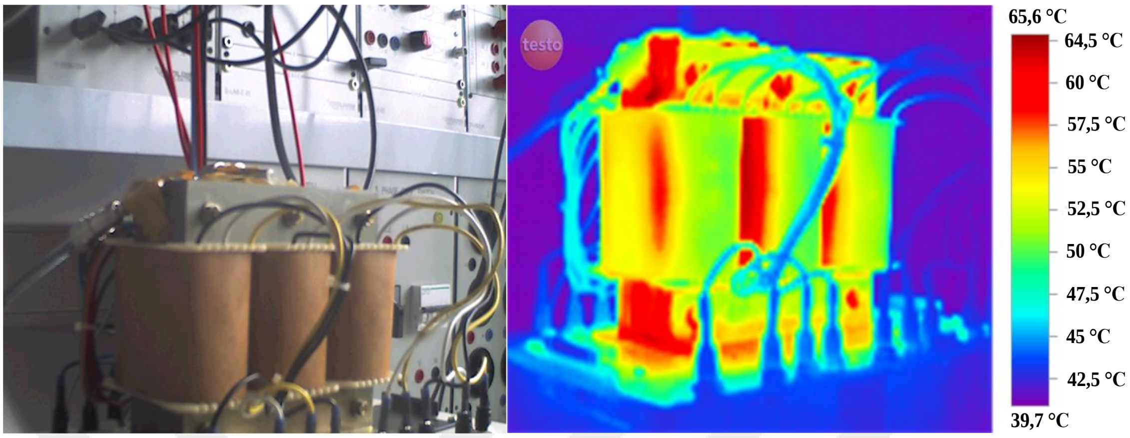

Figure 4.21. Thermal analysis of the transformer by using a thermal imaging camera.

Monitoring of the currents and voltages in the primary and secondary coils of the transformer is realized by using a power analyzer. The transformer currents, voltages, active powers and power losses are observed real-time thanks to an energy analyzer. Primary and secondary voltages and currents signals are monitored via an oscilloscope. As a result, the transformer is tested by setting up an experiment unit in the laboratory. All measurements and signals are measured and compared with the simulation results in order to verify the simulation results of the designed transformer. The block diagram of the experimental setup unit is shown in Figure 4.22.

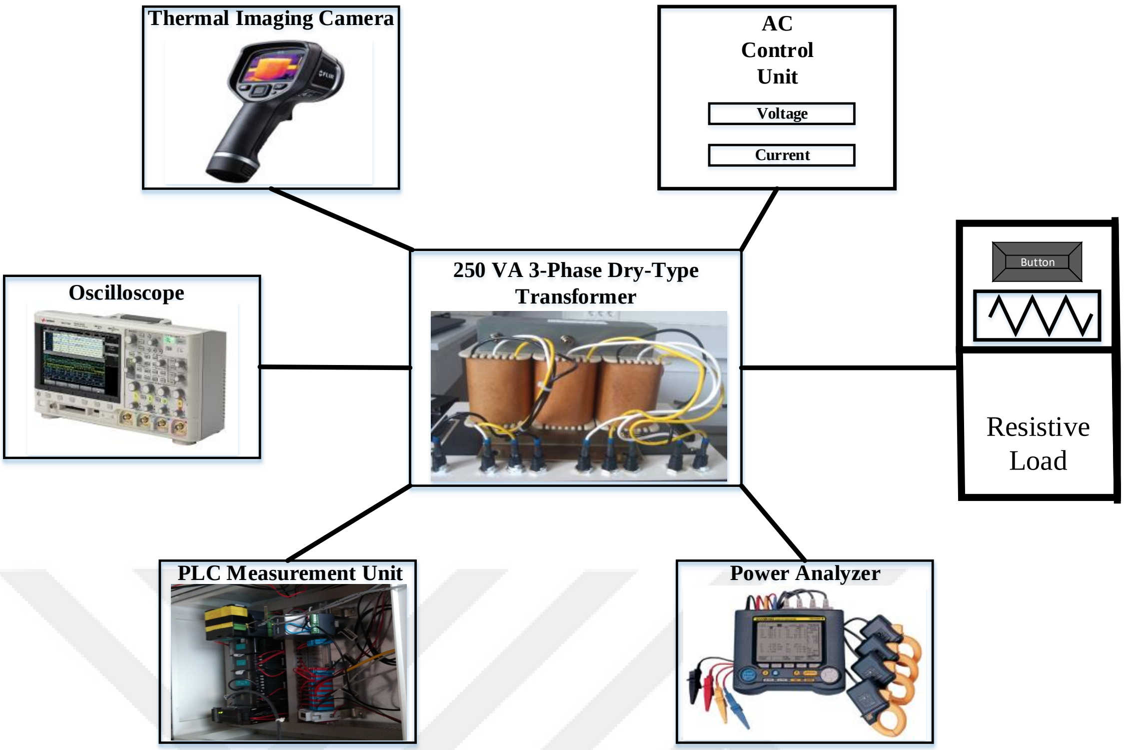

Figure 4.22. The block diagram of the transformer's experimental setup unit.

5. CONCLUSIONS

The dry-type transformers are suitable for indoor and outdoor application and considered to be more efficient, longer lasting and reliable overload capacity. They have many superiorities compared with oil-immersed transformers because of their non-flammable characteristic, better dielectric strength, excellent environmental performance, easy installation and maintenance. However, poor heat conduction performance and limited cooling capacity of dry-type transformers affect their electrical efficiency and working performance seriously. Especially, increasing winding temperature and electrical core losses can cause internal insulation aging and shorten the life span of the transformers under the load and overload condition. Moreover, the dry type transformers need the larger coils compared to oil-filled transformers with the same capacity ratings due to requiring a better insulating system.

The main of this thesis is to present the cost-effective and more efficient 3-phase dry-type transformer model. A 250 VA 380/110-V wye connected 3-phase dry-type transformer is used to reproduce the transformer based on optimum weight-size-efficiency. The transformer parameters are obtained by using a mathematical model and then these parameters are optimized depending on the C (core quality factor) and s (current density of the windings) values in the PSO method. After the optimization process, the transformer is designed by using optimization parameters and then analyzed electromagnetically and thermally. Finally, the optimized transformer is manufactured as optimum size and efficiency. This transformer is also tested and analyzed in the laboratory by using an experimental setup unit. Thus, simulation results are compared with the experimental results to verify the study. These results are presented as follows:

- The core quality factor (C) parameter plays an important role in the efficiency of the transformer. It is shown that this value directly affects power losses on the transformer related to the temperature rises on the core.

- The current density of the windings (s) can be selected by making concessions from the maximum efficiency value or vice versa.

- PSO method has an effective solution for 3-phase dry-type transformer optimization problems. It achieves to obtain personal best and global best values.

- The transformer is analyzed more accurately thanks to the ANSYS/Maxwell program. Because, the simulation results such as the power losses, thermal measurements, magnetic field, coil voltages and currents are verified with the experimental results.

- The temperature measurements are accurately obtained thanks to designed PLC measurement station. The results are also verified by the ANSYS/Maxwell.

- The results show that when the lower and upper limit values of C and s values were selected, the minimum and maximum values of the efficiency and the total weight are obtained at the different C and s values. During the optimization, both minimum weight and maximum efficiency are not obtained at the same time.

6. RECOMMENDATIONS

During the optimization process, the highest efficiency and the lowest weight were obtained at C = 0.7. However, the change in s value shows opposite effects of electrical efficiency and weight. Maximum efficiency is obtained when s is selected at the lower limit value and minimum weight is obtained when s is selected at the upper limit value. Therefore, it is necessary for the designer to decide the s value by considering the economic criteria.

REFERENCES

Abdmouleh, Z., Gastli, A., Ben-Brahim, L., Haouari, M., Al-Emadi, N. A. (2017). Review of optimization techniques applied for the integration of distributed generation from renewable energy sources. *Renewable Energy*, *113*, 266–280.

Aghmasheh, R., Rashtchi, V., Rahimpour, E. (2018). Gray Box Modeling of Power Transformer Windings Based on Design Geometry and Particle Swarm Optimization Algorithm. *IEEE Transactions on Power Delivery*, *33*(5), 2384–2393.

Aksu, İ. Ö., & Demirdelen, T. (2018). A comprehensive study on dry type transformer design with swarm-based metaheuristic optimization methods for industrial applications. *Energy Sources, Part A: Recovery, Utilization, and Environmental Effects*, *40*(14), 1743–1752.

Alcan, Y., Öztürk, A., Özmen, Ö. (2014). *Yer Çekimsel Arama Algoritmasi İle Değişik Çalışma Koşulları İçin Tranformatör Verim Optimizasyonu*. 10. ISITES, Karabük.

Arjona, M. A., Hernandez, C., Escarela-Perez, R., & Melgoza, E. (2014). Thermal analysis of a dry-type distribution power transformer using FEA. *2014 International Conference on Electrical Machines (ICEM)*, 2270–2274.

Azizian, D., Bigdeli, M. (2017). A new cast-resin transformer thermal model based on recurrent neural networks. *Archives of Electrical Engineering*, *66*(1), 17–28.

Azizian, D., Bigdeli, M., Faiz, J. (2016a). Design Optimization of Cast-Resin Transformer Using Nature-Inspired Algorithms. *Arabian Journal for Science and Engineering*, *41*(9), 3491–3500.

Azizian, D., Bigdeli, M., Faiz, J. (2016b). Design Optimization of Cast-Resin Transformer Using Nature-Inspired Algorithms. *Arabian Journal for Science and Engineering*, *41*(9), 3491–3500.

Bagheri, M., Subramaniam, A., Bhandari, S., Chandar, S., Nadarajan, S., Gupta, A. K., Panda, S. K. (2015). Thermal prognosis of dry-type transformer: Simulation study on load and ambient temperature impacts. *IECON 2015 - 41st Annual Conference of the IEEE Industrial Electronics Society*, 001158–001163.

Basak, R., Das, A., Sanyal, A. (2015). Cost Optimal Design of a Single-Phase Dry Power Transformer. *Indonesian Journal of Electrical Engineering and Informatics (IJEEI), 3*(4), 261–266.

Blanco Alonso, P. E., Meana-Fernández, A., Fernández Oro, J. M. (2017). Thermal response and failure mode evaluation of a dry-type transformer. *Applied Thermal Engineering*, *120*, 763–771.

Chitaliya, G. H., Joshi, S. K. (2016). Determination of temperature rise in a dry type transformer using finite element analysis. *2016 IEEE Annual India Conference (INDICON)*, 1–6.

Çelebi, M. (2008). Genetik Algoritma ile Kuru bir Trafonun Maliyet Optimizasyonu. *Eleco*, 189-193.

Del Vecchio, R. M., Poulin, B., Feghali, P. T., Shah, D. M., Ahuja, R. (2017). *Transformer Design Principles (3rd ed.).* Boca Raton London New York Washington, D.C.

Eberhart, R., Kennedy, J. (1995). A new optimizer using particle swarm theory. *MHS'95. Proceedings of the Sixth International Symposium on Micro Machine and Human Science*, 39–43.

Eberhart, Yuhui Shi. (2001). Particle swarm optimization: developments, applications and resources. *Proceedings of the 2001 Congress on Evolutionary Computation (IEEE Cat. No.01TH8546)*, *1*, 81–86.

Engelbrecht, A. P. (2007). *Computational Intelligence: An Introduction*, 2nd ed. Chichester, U.K.: Wiley.

Erdoğmuş, P., Yalçin, E. (2015). Parçacik Sürü Optimizasyonu İle Kisitsiz Optimizasyon Test Problemlerinin Çözümü. *Journal of Advanced Technology Sciences.4(1)*, 14-22.

Eslamian, M., Vahidi, B., Eslamian, A. (2011). Thermal analysis of cast-resin dry-type transformers. *Energy Conversion and Management*, *52*(7), 2479–2488.

Finocchio, M. A. F., Lopes, J. J., de França, J. A., Piai, J. C., Mangili, J. F. (2017). Neural networks applied to the design of dry-type transformers: an example to analyze the winding temperature and elevate the thermal quality: Neural networks applied to the design of dry-type transformers. *International Transactions on Electrical Energy Systems*, *27*(3), e2257.

Fish, J., Belytschko T. (2007). *A First Course in Finite Elements*. John Wiley & Sons Ltd., England.

Ghazizadeh, M., Faiz, J., Oraee, H. (2016). Derating of distribution transformers under non-linear loads using a combined analytical-finite elements approach. *IET Electric Power Applications*, *10*(8), 779–787.

Glotic, A., Sarajlic, N., Kasumovic, M., Tesanovic, M., Sarajlic, M., & Pihler, J. (2016). Identification of thermal parameters for transformer FEM model by differential evolution optimization algorithm. *2016 International Conference Multidisciplinary Engineering Design Optimization (MEDO)*, 1–6.

IEEE. (2006). *IEEE Recommended Practice for Installation, Application, Operation, and Maintenance of Dry-Type General Purpose Distribution and Power Transformers*. https://doi.org/10.1109/IEEESTD.1982.106993

Kalatehjari, R., A Rashid, A. S., Ali, N., Hajihassani, M. (2014). The Contribution of Particle Swarm Optimization to Three-Dimensional Slope Stability Analysis. *The Scientific World Journal*, *2014*, 1–12.

Liu, C., Gong, R., Ruan, J., Liao, C., Wen, W. (2016). Temperature rise of a dry-type transformer with quasi-3D coupled-field method. *IET Electric Power Applications*, *10*(7), 598–603.

Megep. (2011). *BİR FAZLI TRANSFORMATÖR SARIMI*. T.C. MİLLÎ EĞİTİM BAKANLIĞI. 522EE0041, Ankara.

Nabhani, F., Hodgson, S., Warnakulasuriya, K. (2015). *Estimation of Temperature Rise in MVA Range Dry-Type Transformers and Practical Verification Based on Simulated Loading*. *Proceedings of the World Congress on Engineering Proceedings of the World Congress on Engineering 2015 London*, U.K., July 1-3, 2015.

Nochumson, C. J. (2001). Considerations in application and selection of unit substation transformers. *Conference Record of 2001 Annual Pulp and Paper Industry Technical Conference (Cat. No.01CH37209)*, 213–222.

Nunn, T. (2000). A comparison of liquid-filled and dry-type transformer technologies. *2000 IEEE-IAS/PCA Cement Industry Technical Conference. Conference Record (Cat. No.00CH37047)*, 105–112.

Özüpak, Y., MamiŞ, M. S. (2018). *Realization of 3D Electromagnetic and Thermal Analyzes of the Autotransformer by Finite Elements Method*. *7*(7), 6.

Rahimpour, E., Azizian, D. (2007). Analysis of Temperature Distribution in Cast-resin Dry-type Transformers. *Electrical Engineering*, *89*(4), 301–309.

Reddy, J. N., Gartling, D. K. (2010). *The Finite Element Method in Heat Transfer and Fluid Dynamics*. CRC Press Taylor and Francis Group, London, England.

Smajic, J., Franz, T., Bucher, M. K., Limone, A., Shoory, A., Skibin, S., & Tepper, J. (2017). Computational and Experimental Investigation of Distribution Transformers Under Differential and Common Mode Transient Conditions. *IEEE Transactions on Magnetics*, *53*(6), 1–4.

Smolka, J., Nowak, A. J. (2008). Experimental validation of the coupled fluid flow, heat transfer and electromagnetic numerical model of the medium-power dry-type electrical transformer. *International Journal of Thermal Sciences*, *47*(10), 1393–1410.

Soltanbayev, I., Sarmukhanov, R., Kazymov, S., Otelgen, T., Bagheri, M. (2017). Automated Dry-type Transformer Aging Evaluation: A Simulation Study. *International Siberian Conference on Control and Communications*, 6.

Talukder, S. (2011). *Mathematical Modelling and Applications of Particle Swarm Optimization*. Master's Thesis Mathematical Modelling and Simulation Thesis no: 2010:8.

Tokhi, M. O., Alam, M. S. (2015). Particle Swarm Optimisation Algorithms and Their Application to Controller Design for Flexible Structure Systems. *The 1st IEEE International Conference on Computer, Control and Communication (IEEE-IC4), Karachi (Pakistan)*, pp: 7-18.

Tören, M., Çelebi, M. (2016). Impact on efficiency of core materials in dry type transformers. *National Conference on Electrical, Electronics and Biomedical Engineering (ELECO), Bursa, Turkey*, pp. 308-312.

Tsili, M. A., Amoiralis, E. I., Kladas, A. G., Souflaris, A. T. (2012). Power transformer thermal analysis by using an advanced coupled 3D heat transfer and fluid flow FEM model. *International Journal of Thermal Sciences*, *53*, 188–201.

Van den Bergh, F. (2002). *An analysis of particle swarm optimizers*. PhD thesis, Department of Computer Science, University of Pretoria, Pretoria, South Africa.

Wang, S., Wang, Y., Zhao, X. (2015). Calculating model of insulation life loss of dry-type transformer based on the hot-spot temperature. *2015 IEEE 11th International Conference on the Properties and Applications of Dielectric Materials (ICPADM)*, 720–723.

Wu, W., Kern, J. A. (2016). Temperature rise prediction of a natural cooling dry-type transformer. *SoutheastCon 2016*, 1–2.

Xiao, M., Du, B. X. (2016). Effects of high thermal conductivity on temperature rise of epoxy cast winding for power transformer. *IEEE Transactions on Dielectrics and Electrical Insulation*, *23*(4), 2413–2420.

CURRICULUM VITAE

Burak ESENBOĞA was born in Adana, TURKEY, in 1992. He received the B.E. degree in electrical and electronics engineering from the Çukurova University, Adana, Turkey, in 2011. He was the recipient of the Certificate of the top-scoring student in the department at the Çukurova University in 2016. He completed his military training in April 2017. After his military service, he worked on solar photovoltaic systems as an electrical electronics engineer for a year. During his tenure, he managed the installation of a 100 kW solar power plant. He started to study Master of Science in the electric and electronic engineering department, in Adana Alparslan Türkeş Science and Technology University, in 2017, in September. In 2018, March, he joined the Department of Electrical and Electronics Engineering, Adana Alparslan Türkeş Science and Technology University, as a research assistant. He has been with the Department of Electrical and Electronics Engineering Department. His current interests include transformers, solar photovoltaic systems, artificial neural network based optimization, electromagnetic and thermal analysis of the electrical machines.

PROJECTS

The Scientific Project Unit of Adana Science and Technology University, Project Number: 18332006, Modeling and Realization of Dry Type Transformer with Optimum Cost-Size-Efficiency Characteristics, continue, Researcher.

The Scientific Project Unit of Adana Science and Technology University, Project Number: 18103015, A New Method for Generating Short-Term Power Forecasting Based On Artificial Neural Networks and Optimization Methods for Solar Photovoltaic Power Plants, Researcher, 2018.

The Scientific and Technological Research Council of Turkey (TÜBİTAK), Project Number: 118E697, continue, Scholarship Holder.

LIST OF PUBLISHED ARTICLES IN INTERNATIONAL CONFERENCES

ESENBOGA, B., EKINCI, F., KIRMALI, G. (2017) "A Review of Photovoltaic Thermal (PV/T) Modules". Çukurova University, Congress Center, October 25-27, 2017, Adana / TURKEY pp: 1557-1561, Paper ID: 700.,

AYGUL, K., ESENBOGA, B., KAYAALP, R., DEMIRDELEN T., TUMAY M. (2018) "A Comparative Survey of Battery Energy Storage Systems for Renewable Energy Sources". IMCOFE V. International Multidisciplinary Congress of Eurasia. 24-26 July 2018. Barcelona, SPAIN. pp: 435-442.

ESENBOGA, B., AKSU, I.O., AYGUL, K., DEMIRDELEN, T., EKINCI, F. (2018) "Short-Term Generated Power Forecasting Based On Artificial Neural Network in Photovoltaic (PVS) Power Plants". IMCOFE V. International Multidisciplinary Congress of Eurasia. 24-26 July 2018. Barcelona, SPAIN. pp: 410-417.

EKINCI, F., DEMIRDELEN, T., ESENBOGA, B., BILGILI, M., HOPLAMAZ, H. (2018) "Micro-cogeneration Systems Based on Renewable Energy Sources: A General Aspect". GAPYENEV International GAP Renewable Energy and Energy Efficiency Congress. 10-12 May 2018. Şanlıurfa, Turkey.

EKINCI, F., AYGUL, K., ESENBOGA, B., YAVUZDEGER, A., DEMIRDELEN, T. (2019) "Experimental Partial Shading Analysis of Solar Photovoltaic (PV) Panels in Çukurova Region". IMSEC 4th International Mediterranean Science and Engineering Congress. 25-27 April 2019. Alanya, TURKEY. pp: 340.

LIST OF INDEXED CHAPTER IN INTERNATIONAL BOOK CHAPTER

DEMIRDELEN, T., AKSU, I.O., ESENBOGA, B., AYGUL, K., EKINCI F., BILGILI M. (2018) "A New Method for Generating Short-Term Power Forecasting Based On Artificial Neural Networks and Optimization Methods for Solar Photovoltaic Power Plants". SPRINGER NATURE 2018.

LIST OF INDEXED ARTICLE IN INTERNATIONAL JOURNAL

EKINCI, F., DEMIRDELEN, T., AKSU, IO., AYGUL, K., ESENBOGA, B., BILGILI M. (2019) “A Novel Hybrid Metaheuristic Optimization Method to Estimate Medium-Term Output Power for Horizontal Axis Wind Turbine”. Proceedings of the Institution of Mechanical Engineers, Part A: Journal of Power and Energy. 2019 Jan 13;095765091882104.

LIST OF ARTICLES IN NATIONAL CONFERENCES

ESENBOGA, B., AYGUL, K., DEMIRDELEN, T., TUMAY, M. (2018) “2D Finite Element Analysis of a Single Phase Transformer”. CIGRE Turkey National Committee, Power System Conference, 15-16 November 2018. Ankara, TURKEY.

YAVUZDEGER, A., EKINCI, F., ESENBOGA, B., AYGUL, K., DEMIRDELEN, T. (2019) “İçten Yanmalı Motora Dayalı Mikro Kojenerasyon Sisteminin MATLAB/Simulink ile Modellemesi ve Performans Analizi”. XVI. Automatic Control Seminar and Exhibition, 24-25 April 2019, Adana, TURKEY. pp: 146-151.

AYGUL, K., ESENBOGA, B., EKINCI, F., NAZLIGUL, H. (2019) “Kısmi Gölgelenme Durumundaki Fotovoltaik Panellerin Maksimum Güç Noktası Takibi için Sistem Tasarımı ve Kontrolü”. XVI. Automatic Control Seminar and Exhibition, 24-25 April 2019, Adana, TURKEY. pp: 152-157.